LUND UNIVERSITY

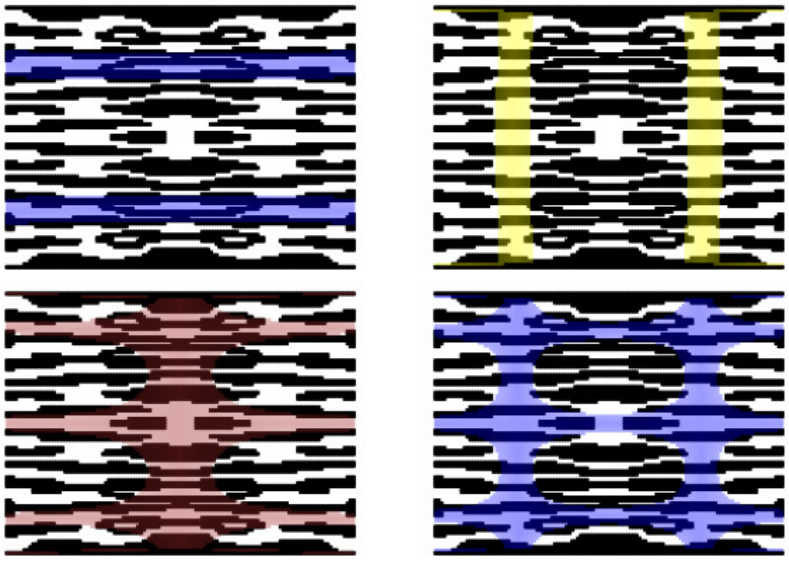

OPTIMIZATION OF ELASTOMER LAYER IN CLT PANELS FOR VIBRATION REDUCTION

NILS ARVIDSSON

Structural Mechanics

Master's Dissertation

DEPARTMENT OF CONSTRUCTION SCIENCES

DIVISION OF STRUCTURAL MECHANICS

ISRN LUTVDG/TVSM--26/5286--SE (1-44) | ISSN 0281-6679

MASTER'S DISSERTATION

OPTIMIZATION OF ELASTOMER LAYER IN CLT PANELS FOR VIBRATION REDUCTION

NILS ARVIDSSON

Supervisor: **LINUS ANDERSSON**, Assistant Professor, Division of Structural Mechanics, LTH.
Assistant Supervisor: Professor **MATHIAS WALLIN**, Division of Solid Mechanics, LTH.
Examiner: **PETER PERSSON**, Associate Professor, Division of Structural Mechanics, LTH.

Printed by V-husets tryckeri LTH, Lund, Sweden, March 2026 *(Pl)*.

For information, address:
Division of Structural Mechanics,
Faculty of Engineering LTH, Lund University, Box 118, SE-221 00 Lund, Sweden.
Homepage: www.byggmek.lth.se

Abstract

In this thesis, optimization of cross-laminated timber panels is performed. A cross laminated timber panel consists of a set of wooden layers, which are bonded together. In this work, a layer of elastomer is included among the wooden layers. As the elastomer is a favourable material to improve the vibrational and acoustic properties, this thesis investigates how this material can be optimally distributed.

The optimization of the panels specifically targets the elastomer layer, by distributing material to regions where it efficiently reduces the vibrational response. The response of the panels is analyzed by loading the panels with a harmonically varying force, where the forcing frequency is varied so that the vibrational response is evaluated over a range of frequencies.

The vibrational response is then used as an objective function in an optimization problem with the constraint functions consisting of a volume constraint of the elastomer and the deflection of the panels due to static loading. As the configuration of the elastomer layer is of interest, topology optimization is employed to find a distribution of elastomer which ultimately yields a lower vibrational response than a uniform layer.

The end result of the elastomer layer shows an interesting pattern where the mode shapes of the panel are reflected in the design, and the response is reduced in the range of $10-20$ %. The potential drawback may be that the eigenvalues appear at a slightly lower frequency.

Acknowledgements

As this thesis is now completed, I would like to express my gratitude to the people involved. Especially Peter for making this thesis possible, as well as for the engaging courses he has taught, Linus for many fruitful discussions and his continuous feedback, which was essential for completing this thesis, and Mathias for his interesting course related to this thesis, and being available for help when needed.

Finally, I would to thank the rest of the teachers at the Division of Structural Mechanics and the Division of Solid Mechanics for providing courses that are not only interesting but also challenging, as this tends to be more rewarding and meaningful.

Contents

1 Introduction

In this thesis, optimization of wooden floor structures is performed. The floor structure is in the form of Cross-Laminated panels. These panels are constructed by wooden layers glued together. For this thesis, these panels also include a layer of an elastomer, which is a rubber like material. The optimization specifically targets the configuration of that layer. The aim is to improve vibrational and acoustic performance. To this end, the panels are loaded by a harmonically varying force in a range of loading frequencies. The overall response in the frequency range is then reduced by removing parts of the elastomer layer.

1.1 Background

As the demands on reducing climate impact of buildings raise, the interest of using wood as a construction material increases, as this is often considered an environmental friendly material. A common wooden floor structure is Cross Laminated Timber (CLT). A CLT panel consist of solid wood laminate glued together in layers. An example of an CLT panel is shown in Figure 1. Each layer is oriented with the wooden fibers orthogonal to the layer above and underneath. The number of layers is always odd so that the stronger fiber direction of the wood is in the same direction for the top and bottom layer with the result that the bending stiffness is larger in one of the directions.

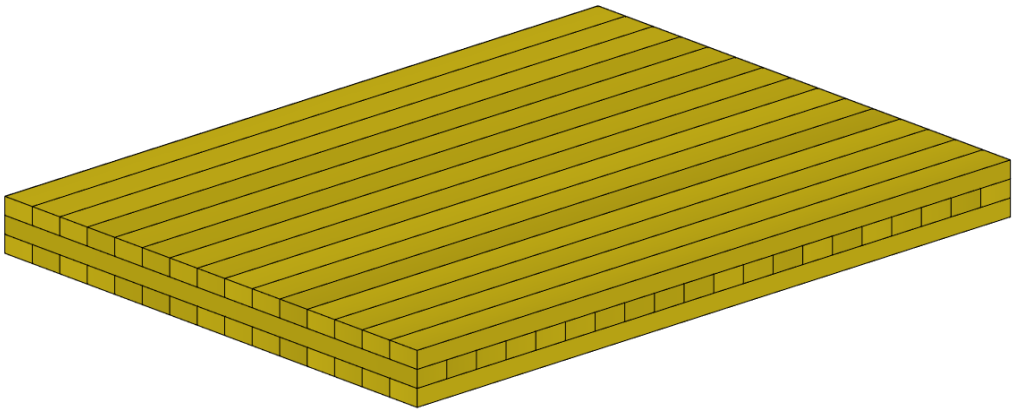

Figure 1: *Example of an CLT panel with 3 layers*

A problem for these panels can be the vibrational and acoustic performance, especially at lower frequencies. Insertion of an elastomer layer between two wood layers in a CLT panel has shown to improve the acoustic performance (Ljunggren 2023). The elastomer is a material with rubber like material parameters and an example of an elastomer layer in a CLT panel could appear as in Figure 2.

Figure 2: *Example of a section of a CLT panel with elastomer layer*

1.2 Aim and objectives

The vibrational and acoustic performance is often evaluated by a frequency response function (FRF). An FRF shows the steady state response of the structure when loaded in a certain frequency range. The steady state response is the response when the structure is excited by a harmonic force and response due to initial excitations has been damped out so that the response also varies harmonic. This is then evaluated at several discrete points over a frequency range, so that an FRF can be established. An example of an FRF is shown in Figure 3.

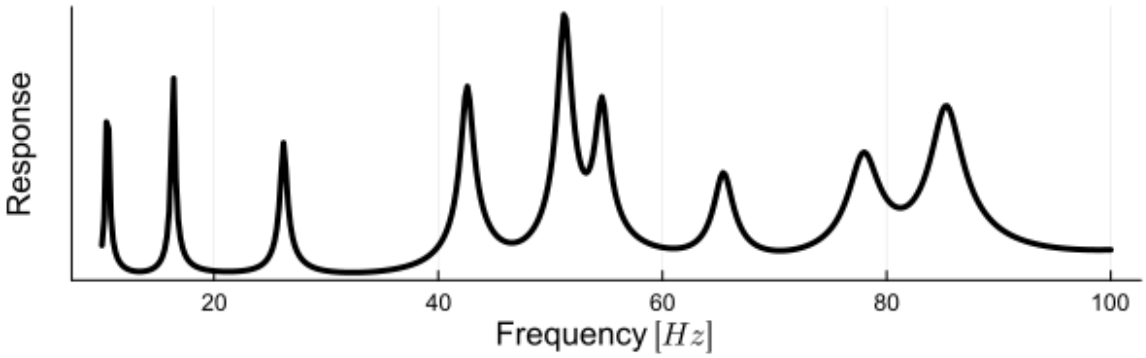

Figure 3: *Example of an FRF in the range of 10 to 100 Hz*

As the elastomer is about to improve the acoustic performance, this raises the question of how it can be utilized the most. Is a full layer with even thickness (a uniform layer) the most favorable or can the dynamic response be reduced further by reallocating the elastomer in a clever way. For instance making the elastomer layer thicker but keeping the volume of the elastomer constant so that void areas are formed.

This thesis aims at finding a suitable distribution of elastomer in that layer, i.e. where should the elastomer be located to reduce the response most. To find such a distribution, the Finite Element Method is used to describe the response of the panels and Topology Optimization is utilized to optimize the elastomer layer. An objective function will be formed, describing the response of the panel when it is loaded over a frequency span. The objective function is subject to the constraint functions, volume restriction of the elastomer and the stiffness of the CLT panel when loaded by a static force. From those functions an optimization problem can be formulated where the aim is to minimize the objective similar to Figure 4.

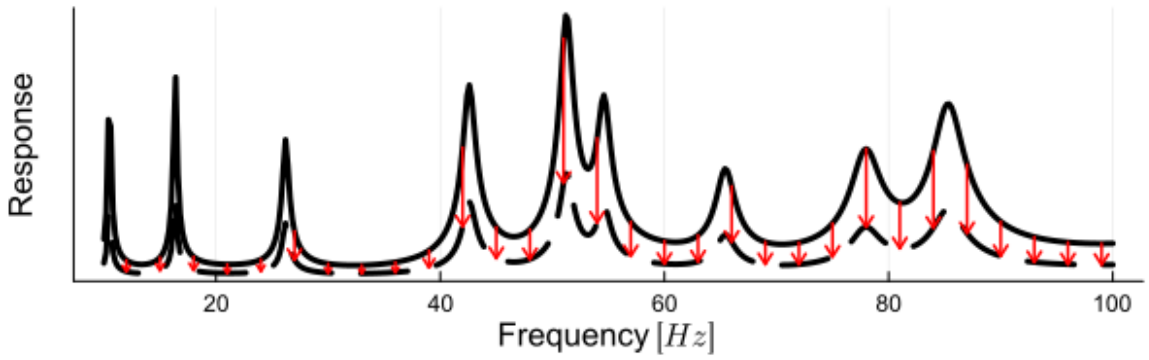

Figure 4: *Aim of this thesis - Reducing vibrational response of CLT-panels.*

1.3 Limitations

This thesis is limited to numerical calculations, experiments has not been carried out to verify the results. The result presented is not to be seen as panels which are ready for use. The dimensions presented may not even be realistic for use as a bearing floor construction. The purpose is to present how an optimized design may appear and how such a design may be obtained. Furthermore, the modelling consider only small deformations along with linear material response. As the elastomer posses viscoelastic properties this is thereby neglected. The size of the finite element discretization has not been verified to be sufficient small for the frequency span considered. The size has been chosen to be as small as the computational power used has allowed for, so that a fine resolution for the optimized layer has been obtained. The wood in the panels is only modelled with respect to two directions - fiber direction and orthogonal to fiber. The response of the panels is only evaluated based on acceleration.

2 Theory

In this section the fundamental theory and equations needed to optimize the panels is briefly presented. The basis is the Finite Element method used to describe the mechanical behavior of the panels. This is followed by a section of structural optimization theory, containing some basic theory describing how an optimization problem can be formed and solved. Finally, a brief description of structural dynamics are presented, which is needed to analyze the response of the panels and to formulate the objective function.

2.1 Finite Element Method

The Finite Element (FE) Method is a solution method to various differential equations, especially useful when an analytical solution is too complicated. The solution procedure starts with a physical relation, for instance Newtons second law, which is used to form the strong form, valid in all material points. This is then relaxed by integrating over a region so that the weak form can be established. The design domain is then discretized, divided into elements where each element has a set of nodes, and each node has a number of *degrees of freedoms* (dofs), used to describe a quantity. The quantities are interpolated between the nodes by the use of shape functions. The discretized domain, consisting of small elements can then be assembled into a global equation system. When this is solved, the value of the quantity at each dofs is obtained.

2.1.1 Strong and weak form

The balance of linear momentum of a material point can be described by Cauchy's equation of motion with cartesian index notation

$$\sigma_{ij,j} + \rho b_i = \rho a_i \tag{1}$$

where σ_{ij} is a symmetric ($\sigma_{ij} = \sigma_{ji}$) stress tensor and b_i is the body force, ρ is the density and a_i is the acceleration. To derive the weak form, the approach used in (Ottosen and Petersson 1992) will be followed and is therefore referred to for a more detailed description.
By introducing the differential operator $\tilde{\nabla}$

$$\tilde{\nabla}^T = \begin{bmatrix} \frac{\partial}{\partial x} & 0 & 0 & \frac{\partial}{\partial y} & \frac{\partial}{\partial z} & 0 \\ 0 & \frac{\partial}{\partial y} & 0 & \frac{\partial}{\partial x} & 0 & \frac{\partial}{\partial z} \\ 0 & 0 & \frac{\partial}{\partial z} & 0 & \frac{\partial}{\partial x} & \frac{\partial}{\partial y} \end{bmatrix}$$

and defining the body force $\boldsymbol{b}$ and acceleration $\boldsymbol{a}$ vectors, and using symmetry to formulate the stress $\boldsymbol{\sigma}$ in voigt format,

$$\boldsymbol{b} = \begin{bmatrix} b_x \\ b_y \\ bz \end{bmatrix}, \quad \boldsymbol{a} = \begin{bmatrix} a_x \\ a_y \\ a_z \end{bmatrix}, \quad \boldsymbol{\sigma} = \begin{bmatrix} \sigma_{xx} \\ \sigma_{yy} \\ \sigma_{zz} \\ \sigma_{xy} \\ \sigma_{xz} \\ \sigma_{zy} \end{bmatrix}$$

allows equation (1) to be written as follows:

$$\tilde{\nabla}\boldsymbol{\sigma} + \rho\boldsymbol{b} = \rho\boldsymbol{a} \tag{2}$$

which is referred to as the strong form. To derive the weak form, equation (2) is multiplied with an arbitrary vector $\boldsymbol{v} = [v_x \quad v_y \quad v_z]^T$ and integrated over the region V.

$$\int_V \boldsymbol{v}\tilde{\nabla}\boldsymbol{\sigma}\mathrm{d}V + \int_V \boldsymbol{v}\rho\boldsymbol{b}\mathrm{d}V = \int_V \boldsymbol{v}m\boldsymbol{a}\mathrm{d}V \tag{3}$$

Using Green-Gauss theorem $\int_V \phi\mathrm{div}(\boldsymbol{q})\mathrm{d}V = \int_S \phi\boldsymbol{q}^T n\mathrm{d}S - \int_V(\nabla\phi)^T\boldsymbol{q}\mathrm{d}V$ where $\boldsymbol{q}$ is an arbitrary vector, $\phi = \phi(x, y, z)$ is an arbitrary function and $\boldsymbol{n} = [n_x \quad n_y \quad n_z]^T$ being the unit normal vector. The weak form can be formed:

$$\int_V (\tilde{\nabla}v)^T\boldsymbol{\sigma}\mathrm{d}V + \int_V \rho\boldsymbol{v}^T\boldsymbol{a}\mathrm{d}V = \int_S \boldsymbol{v}^T\boldsymbol{t}\mathrm{d}S + \int_V \boldsymbol{v}^T\boldsymbol{b}\mathrm{d}V \tag{4}$$

Where $\boldsymbol{t} = [t_x \quad t_y \quad t_z]^T = t_i = \sigma_{ij}n_j$ is a traction vector which appears as a natural boundary condition (Neumann) for the force on the surface of the body.

2.1.2 Constitutive relation

The constitutive relation is the relation between stresses and strains, and for a linear elastic material the stress strain relation can be written $\boldsymbol{\sigma} = \boldsymbol{D}\boldsymbol{\epsilon}$. If the strains $\boldsymbol{\epsilon}$ is formulated according to equation (5), the compliance matrix $\boldsymbol{C}$ may be written as equation (6) (Ottosen and Ristinmaa 2005), for an orthotropic material which has three symmetry planes where $\boldsymbol{C} = \boldsymbol{D}^{-1}$.

$$\boldsymbol{\epsilon} = \begin{bmatrix} \epsilon_{xx} \\ \epsilon_{yy} \\ \epsilon_{zz} \\ 2\epsilon_{xy} \\ 2\epsilon_{xz} \\ 2\epsilon_{yz} \end{bmatrix} \tag{5}$$

$$\begin{bmatrix} \epsilon_{xx} \\ \epsilon_{yy} \\ \epsilon_{zz} \\ 2\epsilon_{xy} \\ 2\epsilon_{xz} \\ 2\epsilon_{yz} \end{bmatrix} = \begin{bmatrix} 1/E_x & -\nu_{yx}/E_y & -\nu_{zx}/E_z & 0 & 0 & 0 \\ -\nu_{xy}/E_x & 1/E_y & -\nu_{32}/E_z & 0 & 0 & 0 \\ -\nu_{xz}/E_x & -\nu_{yz}/E_y & 1/E_z & 0 & 0 & 0 \\ 0 & 0 & 0 & 1/G_{xy} & 0 & 0 \\ 0 & 0 & 0 & 0 & 1/G_{xz} & 0 \\ 0 & 0 & 0 & 0 & 0 & 1/G_{yz} \end{bmatrix} \begin{bmatrix} \sigma_{xx} \\ \sigma_{yy} \\ \sigma_{zz} \\ \sigma_{xy} \\ \sigma_{xz} \\ \sigma_{yz} \end{bmatrix} \tag{6}$$

Here, E is young's modulus, G is the shear modulus and ν is Poisson's ratio. The matrix $\boldsymbol{C}$ can be shown to be symmetric and therefore

$$\nu_{yx}/E_y = \nu_{xy}/E_x \qquad \nu_{zx}/E_z = \nu_{xz}/E_x \qquad \nu_{32}/E_z = \nu_{yz}/E_y$$

which means there are nine independent material parameters in an orthotropic material. If there exists a plane of isotropy in an orthotropic material it is referred to as transversal isotropy (Ottosen and Petersson 1992). If that plane is the $y - z$ and letting it be denoted by subscript t, so that $E_y = E_z = E_t$, $G_{xy} = G_{xz} = G_{xt}$, and the shear modulus in the transversal $x - y$ plane is given by $G_t = E_t/(2(1 + v_t))$

because of isotropy in that plane, there are then 5 independent material parameters. The compliance matrix is then formulated as:

$$\boldsymbol{C} = \begin{bmatrix} 1/E_x & -\nu_{tx}/E_t & -\nu_{tx}/E_t & 0 & 0 & 0 \\ -\nu_{xt}/E_x & 1/E_t & -\nu_t/E_t & 0 & 0 & 0 \\ -\nu_{xt}/E_x & -\nu_t/E_t & 1/E_t & 0 & 0 & 0 \\ 0 & 0 & 0 & 1/G_{xt} & 0 & 0 \\ 0 & 0 & 0 & 0 & 1/G_{xt} & 0 \\ 0 & 0 & 0 & 0 & 0 & 2(1+\nu_t)/E_t \end{bmatrix}$$

If the material is isotropic there are only two independent material parameters and the compliance matrix is given by:

$$\boldsymbol{C} = \frac{1}{E} \begin{bmatrix} 1 & -\nu & -\nu & 0 & 0 & 0 \\ -\nu & 1 & -\nu & 0 & 0 & 0 \\ -\nu & -\nu & 1 & 0 & 0 & 0 \\ 0 & 0 & 0 & 2(1+\nu)/E & 0 & 0 \\ 0 & 0 & 0 & 0 & 2(1+\nu)/E & 0 \\ 0 & 0 & 0 & 0 & 0 & 2(1+\nu)/E \end{bmatrix}$$

2.1.3 Finite Element discretization

To derive the Finite element form, the weak form and the constitutive relation is repeated here for convenience:

$$\int_V (\tilde{\nabla}\boldsymbol{v})^T \boldsymbol{\sigma} \mathrm{d}V + \int_V \rho \boldsymbol{v}^T \boldsymbol{a} \mathrm{d}V = \int_S \boldsymbol{v}^T \boldsymbol{t} \mathrm{d}S + \int_V \boldsymbol{v}^T \boldsymbol{b} \mathrm{d}V$$
$$\boldsymbol{\sigma} = \boldsymbol{D}\boldsymbol{\epsilon}$$

Considering small deformations the strains can be written as: (Ottosen and Petersson 1992).

$$\boldsymbol{\epsilon} = \tilde{\nabla}\boldsymbol{u}$$

The displacement vector $\boldsymbol{u}$ and acceleration vector $\ddot{\boldsymbol{u}}$ is approximated by $\boldsymbol{u} = \boldsymbol{N}\boldsymbol{x}$ and $\ddot{\boldsymbol{u}} = \boldsymbol{N}\ddot{\boldsymbol{x}}$. $\boldsymbol{N}$ holds the shape function which interpolates the nodal displacement $\boldsymbol{x}$ and acceleration $\ddot{\boldsymbol{x}}$. Using Galerkin method the arbitrary vector $\boldsymbol{v}$ is chosen as $\boldsymbol{v} = \boldsymbol{N}\boldsymbol{c}$. This allows the weak form to be rewritten as a finite element formulation:

$$\int_V \boldsymbol{B}^{\boldsymbol{T}} \boldsymbol{D} \boldsymbol{B} \mathrm{d}V \boldsymbol{x} + \rho \int_V \boldsymbol{N}^{\boldsymbol{T}} \boldsymbol{N} \mathrm{d}V \ddot{\boldsymbol{x}} = \underbrace{\int_{\partial S_N} \boldsymbol{N}^{\boldsymbol{T}} \boldsymbol{t} \mathrm{d}S}_{\boldsymbol{f^t}} + \underbrace{\int_{\partial S_D} \boldsymbol{N}^{\boldsymbol{T}} \boldsymbol{t_D} \mathrm{d}S}_{\boldsymbol{f^r}} + \underbrace{\int_V \boldsymbol{N}^{\boldsymbol{T}} \boldsymbol{b} \mathrm{d}V}_{\boldsymbol{f^b}} \quad (7)$$

To account for boundary condition the surface S is split in two terms where Neumann boundary conditions is applied as a traction $\boldsymbol{t}$ on ∂S_N and Dirichlet boundary is applied on ∂S_D where displacement is prescribed and reaction forces $\boldsymbol{f^r}$ can be obtained after solving the global system. In this thesis, the discretization of the design domain is divided into hexahedron shaped element where each element has eight nodes, one in each of the vertices. Each node then has three dofs so that a vector valued interpolation is done. The interpolation is done by using Lagrangian shape functions. And the integration of equation (7) is done over each element. Each element integral is evaluated by numerical integration with $2 \times 2 \times 2$ Gauss points to form element

matrices. These element matrices are then assembled into a global system. Using $\mathbb{A}$ as an assembly operator, the local element matrices are assembled into the global system, where the stiffness matrix $\boldsymbol{K}$, mass matrix $\boldsymbol{M}$ and force vector $\boldsymbol{f}^I$ are given as:

$$\boldsymbol{K} = \mathop{\mathbb{A}}_{e \in W} \underbrace{\int_V \boldsymbol{B_e}^{\boldsymbol{T}} \boldsymbol{D_e^w} \boldsymbol{B_e} dV}_{\boldsymbol{k_e^w}} + \mathop{\mathbb{A}}_{e \in EL} \underbrace{\int_V \boldsymbol{B_e}^{\boldsymbol{T}} \boldsymbol{D^{el}} \boldsymbol{B_e} dV}_{\boldsymbol{k_e^{el}}}$$

$$\boldsymbol{M} = \mathop{\mathbb{A}}_{e \in W} \underbrace{\int_V \rho^w \boldsymbol{N_e}^{\boldsymbol{T}} \boldsymbol{N_e} dV}_{\boldsymbol{m_e^w}} + \mathop{\mathbb{A}}_{e \in EL} \underbrace{\int_V \rho^{el} \boldsymbol{N_e}^{\boldsymbol{T}} \boldsymbol{N_e} dV}_{\boldsymbol{m_e^{el}}}$$

$$\boldsymbol{f}^I = \mathop{\mathbb{A}}_{e \in W \cup EL} \left(\boldsymbol{f_e^t} + \boldsymbol{f_e^b} \right)$$

Where W is the set of elements that belong to wood, EL belong to the elastomer layer and is the elements where the optimization later will be implemented. ρ^w and ρ^{el} is the density for wood and elastomer. $\boldsymbol{D}^w$ is the transversal isotropic stiffness matrix, which is chosen so that the fiber direction of wood is oriented correctly. $\boldsymbol{D}^{el}$ is the isotropic stiffness matrix of the elastomer layer. The equation system can then be formed as:

$$\boldsymbol{K}\boldsymbol{x} + \boldsymbol{M}\ddot{\boldsymbol{x}} = \boldsymbol{f}^I$$

2.2 Structural optimization

Structural optimization can be divided in three main categories. Size-, shape- and topology optimization. Size optimization optimizes the size of different parts of a structure, for instance the bars in a truss. Shape optimization lets the boundaries of a design domain be controlled by the design variables. Topology optimization consist of letting the design variables control the element matrices of a structure, i.e. where to have material and where not to. For this thesis, topology optimization is used.

Structural optimization problems and in particular topology optimization problems usually consist of a large set of design variables. A suitable solution method for such a problem is Lagrangian Duality.

$$\min_{z \in \chi} \max_{\boldsymbol{\lambda} \geqslant \boldsymbol{0}} \mathcal{L}(\boldsymbol{z}, \boldsymbol{\lambda})$$

$$\mathcal{L}(\boldsymbol{z}, \boldsymbol{\lambda}) = g_0(\boldsymbol{z}) + \sum_{i=1}^{l} \lambda_i g_i(\boldsymbol{z})$$

Where

$$\chi = \left\{ \boldsymbol{z} \in \mathbb{R}^n : z_j^{min} \leqslant z_j \leqslant z_j^{max}, j = 1, ..., n \right\}$$

and g_0 being the objective function subject to l constraint functions g_i and $z_j^{min} = 0$, $z_j^{max} = 1$ being the lower and upper limit on the design variables $\boldsymbol{z}$. $z_j = 0$ corresponds to that element j is void, and if we have $z_j = 1$ there is material in element j. Intermediate values are somewhere in-between, which may not be realistic from a physical point of view. This issue is further discussed in Section 2.2.2 and 2.2.3

To use Lagrangian duality, the problem needs to be convex and separable. That it is separable means that it can be written as a sum of functions of a single variable, thus instead of solving a large problem of a large set of variables, a single variable problem can be solved for each design variable. Topology optimization problem is generally

nonconvex. To tackle this, a convex approximation can be made, which can be solved to find a new design. This can be repeated until the solution has converged and a minimum has been found. As the problem itself is nonconvex it can not be guaranteed that a global minimum is found.

2.2.1 Methods of Moving Asymptotes

The convex approximation used in this thesis is the Method of Moving Asymptotes (MMA) developed by (Svanberg 1987). Besides being convex and separable, this approximation has the benefit of controlling how conservative it is based on the convergence rate. If the convergence is too slow, it is made less conservative and if it does not converge at all, the approximation is made more conservative.
The MMA is based on a first order taylor expansion around the current design denoted with a supscript k and the approximation of g_i, $i = 0, 1, 2..., l$ yields:

$$g_i^{M,k}(\boldsymbol{z}) = r_i^k + \sum_{j=1}^{n} \left(\frac{p_{ij}^k}{U_j^k - z_j} + \frac{q_{ij}^k}{z_j - L_j^k} \right)$$

$$p_{ij}^k = \begin{cases} (U_j^k - z_j^k)^2 \frac{\partial g_i(\boldsymbol{z}^k)}{\partial x_j} & \text{if} \quad \frac{\partial g_i(\boldsymbol{z}^k)}{\partial z_j} > 0 \\ 0 & otherwise. \end{cases}$$

$$q_{ij}^k = \begin{cases} 0 & \text{if} \quad \frac{\partial g_i(\boldsymbol{z}^k)}{\partial z_j} \leqslant 0 \\ -(z_j^k - L_j^k)^2 \frac{\partial g_i(\boldsymbol{z}^k)}{\partial x_j} & otherwise. \end{cases}$$

$$r_i^k = g_i(\boldsymbol{z}^k) - \sum_{j=1}^{n} \left(\frac{p_{ij}^k}{U_j^k - z_j^k} + \frac{q_{ij}^k}{z_j^k - L_j^k} \right)$$

$$L_j^k < z_j^k < U_j^k$$

Where L and U are the lower and upper asymptotes which are updated based on convergence history. If the convergence is slow they are put further away from the design variable z_j^k to make the approximation less conservative. If the design variable oscillates and do not converge, the approximation is made more conservative by putting the asymptote closer to the design variable. For a more detailed explanation about the updating procedure or MMA in general, see (Christensen et al. 2009) or (Svanberg 1987). The latter has distributed an MMA solver which has been used for this thesis.

As the approximation is based on the current design, it is implied that there must be an initial design of the structure, and how this is chosen may affect the end result.

To conclude this section we note that the objective and the constraint functions needs to be evaluated each iteration, along with their partial derivatives with respect to each design variable.

2.2.2 Penalization

The lower and upper bounds on the design variables is set to $z_j^{min} = 0$ and $z_j^{max} = 1$, however there is nothing that says that intermediate values can not occur. These intermediate values can be favorable in a numerical model, but from a physical point of view, intermediate values can not be accepted in the final design. This would for

example imply that for an element, which has a value of the design variable of 0.5, would possess values of stiffness, damping and mass which are half of the values for the elastomer considered. That would imply that a different material is obtained. Therefore, a penalization scheme must be used so that the final converged design has discrete values of 1 (elements where there are material) or 0 (elements without material), this is commonly referred to as a black and white design. To achive this a SIMP-scheme (solid isotropic material penalization) (Christensen et al. 2009) is used where the filtered design variable is raised to a value of p, q, r respectively when assembling the stiffness, mass and damping matrix. Damping will be introduced in Section 2.3.3.

2.2.3 Filtering of the design variables

Filtering is done to avoid oscillations of the design variables between neighboring elements, which can result in a checkerboard design pattern which may result in a design that is only numerical stiff. PDE filter has been used where the relation between the design variables $\boldsymbol{z}$ and the filtered design variables $\tilde{\boldsymbol{\kappa}}$ is described by the partial differential equation $-l_o^2\nabla\tilde{\kappa} + \tilde{\kappa} = z$, where l_o controls the filtering radius. The FE formulation is given by $(l_o^2\boldsymbol{K_f} + \boldsymbol{M_f})\tilde{\boldsymbol{\kappa}} = \boldsymbol{T}_N\boldsymbol{z}$. This is described further in (Lazarov et al. 2011) and (Wallin et al. 2020). In this thesis, the filter has been implemented over a symmetry quarter of the design domain (i.e. a quarter of the elastomer layer in Figure 9 and 17).

The matrices are assembled according to:

$$\boldsymbol{K}_f = \mathop{\mathbb{A}}_{e\in ELq}\int_A \boldsymbol{B}_{\boldsymbol{e}}^T\boldsymbol{B}_{\boldsymbol{e}}dA$$
$$\boldsymbol{M}_f = \mathop{\mathbb{A}}_{e\in ELq}\int_A \boldsymbol{N}_{\boldsymbol{e}}^T\boldsymbol{N}_{\boldsymbol{e}}dA$$

where ELq is a set which is the symmetry quarter of the elastomer elements, and $\boldsymbol{N}$ are the shape functions with scalar valued interpolation, and $\boldsymbol{B}$ is the gradients of the shape functions. $\boldsymbol{T}_N$ transforms $\boldsymbol{z}$ to nodal values so that filtering can be performed by

$$\tilde{\kappa} = \underbrace{\boldsymbol{T}_E(l_o^2\boldsymbol{K}_f + \boldsymbol{M}_f)^{-1}\boldsymbol{T}_N}_{\boldsymbol{A}_f}\boldsymbol{z} \tag{8}$$

where $\boldsymbol{T}_E$ average nodal values to element values. When the design is filtered there will be areas between void and filled where the design variables do not belong to 1 or 0, but instead will be somewhere in-between (gray areas). The remedy for this, to achieve a black and white design, thresholding are performed on the design variables by using a heaviside step function H, see for example (Wang et al. 2011).

$$\kappa_e = \mathrm{H}(\tilde{\kappa}_e, \beta, \eta) = \frac{\tanh\beta\eta + \tanh\beta(\tilde{\kappa}_e - \eta)}{\tanh\beta\eta + \tanh\beta(1-\eta)} \tag{9}$$

Where η is the value which controls if $\tilde{\kappa}$ is projected to a lower or a higher value, and β controls how far the design variables are projected.

2.3 Structural dynamics

We are interested in how the structure response at different forcing frequencies, this is done by load the structure with a harmonic varying force and evaluating the response. The loading frequency can then be changed to evaluate different frequencies, or a frequency span. In this section, details on how the structure is loaded and how the response is evaluated will be described, starting with a single degree of freedom system (sdof). As the final structure to be solved needs multiple degrees of freedoms to be described sufficiently, it might seem redundant to describe a sdof system. The purpose of doing so is that the principal behavior of a sdof system applies to a mdof (multiple degree of freedom) system, and a mdof system may be treated as a sum of sdof systems, this is achieved by the means of modal analysis.

2.3.1 Rotating Vectors

To describe a harmonic time dependent function a set of sine and cosine functions may be used. For large systems, the use complex rotating vectors can further simplify the solution procedure. Rotating complex vector can be described by equation (10), with i being the imaginary unit, t is the time, and ω is the angular frequency. The relation is called Euler's Identity.

$$e^{i\omega t} = \cos(\omega t) + i\sin(\omega t) \tag{10}$$

To show the principle, $f(t) = e^{i\omega t}$ is plotted in Figure 5 with $\omega = 2\pi$. The rotating

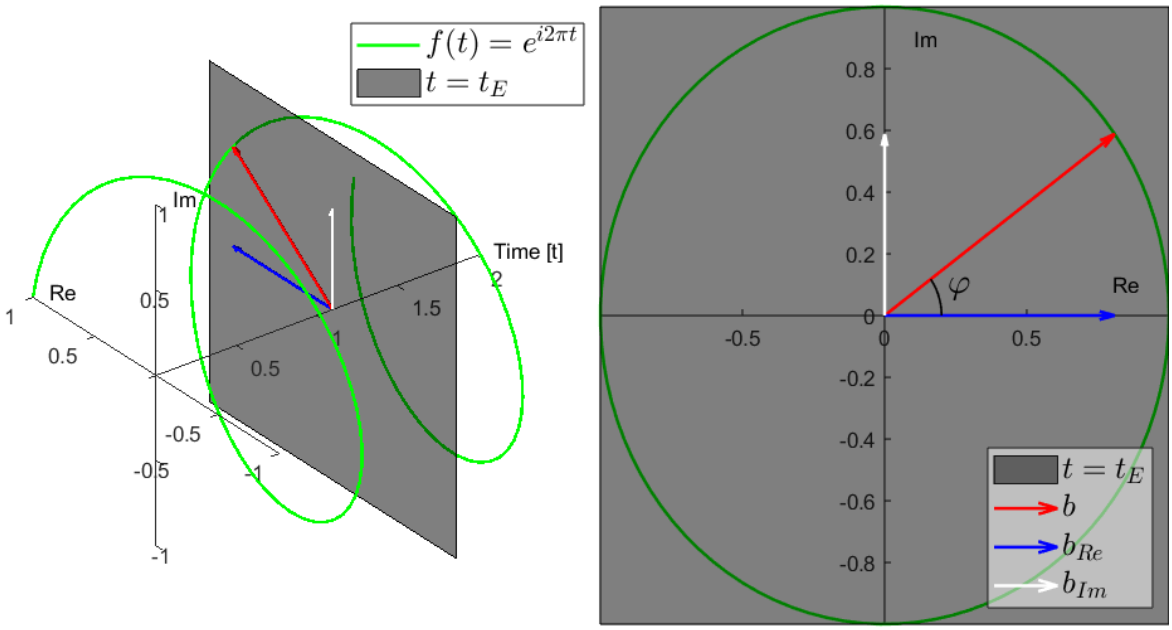

Figure 5: *The principle of rotating vectors. $f(t)$ is plotted in the left figure, with a complex plane at $t = t_E$, shown in the right figure.*

vector in Figure 5 is vector b. Vector b consist of a real part and an imaginary part, shown as $b = b_{Re} + b_{Im}$ in Figure 5. Where $b_{Re} = \mathrm{Re}(f(t)) + 0i$ and $b_{Im} = 0 + i\mathrm{Im}(f(t))$ The complex vector b can also be written $b = \mathrm{Re}(f(t)) + i\mathrm{Im}(f(t))$ with the phase angle $\varphi = tan^{-1}\frac{\mathrm{Im}(f(t))}{\mathrm{Re}(f(t))}$. The real value of f at time t can be retrieved by $\mathrm{Re}(f(t))$. To obtain

the largest value of $f(t)$, the length of vector b is of interest:

$$|b| = \sqrt{b_{Re}^2 + b_{Im}^2} = \sqrt{b\bar{b}}$$

where overline denotes the complex conjugate. If a vector $\boldsymbol{d}$ holds a set of complex numbers, and we are interested in the largest value of each individual complex number. The sum of their squared length d_L, can be obtained by the use of the scalar product.

$$d_L = \boldsymbol{d}^H \boldsymbol{d}$$

Where supscript H is the complex conjugate transpose (Hermitian).

2.3.2 Single degree of freedom

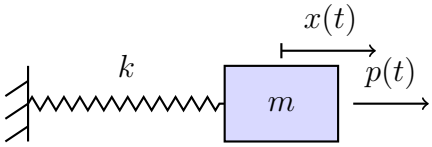

Figure 6: *Figure of a sdof system*

In Figure **??** a single degree of freedom system is shown, consisting of a body with a mass m, connected to a massless spring with stiffness k. The body is loaded with a harmonically varying force p, dependent of time t. The displacement of the body is x. According to Newton's second law such a system is described by the equilibrium equation:

$$m\ddot{x} + kx = p(t) \tag{11}$$

If $p = 0$ and the body is released from rest, we have free vibrations and a solution on the form $C\sin(\omega_n t + \theta)$ where C, θ are constants depending on the initial conditions and $\omega_n = \sqrt{k/m}$ is the eigenfrequency. If the body were to be set into motion it would according to equation (11) go on forever. As a real system always has some sort of energy dissipation, damping needs to be included in the equation. This is typically achieved by adding a viscous damping constant c, being multiplied with the velocity $\dot{x}$.

$$m\ddot{x} + c\dot{x} + kx = p(t) \tag{12}$$

As we are only interested in steady state response (when initial free vibrations has been damped out), we solve for the particular solution of equation (12) which can be assumed to be $x = ue^{i\omega t}$, and as the force varies harmonically $p = \hat{p}e^{i\omega t}$, we obtain

$$(k - \omega^2 m + i\omega c)ue^{i\omega t} = \hat{p}e^{i\omega t}$$

which we can solve for u, as:

$$u = \frac{\hat{p}}{k - \omega^2 m + i\omega c}$$

By insert a damping ratio $\zeta = \frac{c}{2m\omega_n}$, dividing with the static deformation, and taking the amplitude of the expression, the deformation response factor R_d (Chopra 2020) is obtained:

$$R_d = \left|\frac{u}{\hat{p}/k}\right| = \frac{1}{\sqrt{(1 - (\omega/\omega_n)^2)^2 + (2\zeta\omega/\omega_n)^2}} \tag{13}$$

equation (13), representing a response function, is plotted in Figure **??** together with its phase angle φ and different values of ζ.

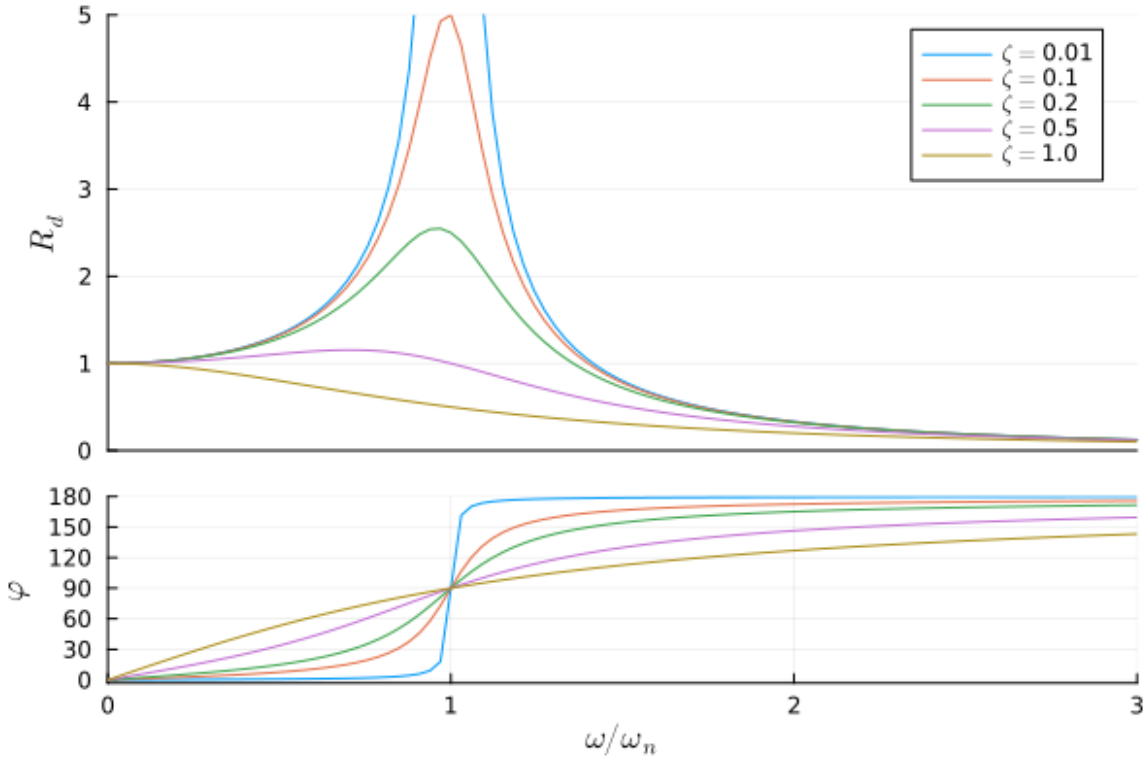

Figure 7: *Response function with different damping ratios, plotted together with the phase angle φ*

From Figure **??** it can be seen that the response amplitude at ω/ω_n (when the loading frequency coincides with the natural frequency of the system) is controlled by the damping ratio, if damping were to be excluded the response would tend to infinity. It can also be seen that the phase angle is 90 degrees, i.e., when the force reaches its maximum the displacement reaches its minimum (so if the force being applied as real, the displacement would be imaginary).

2.3.3 Multiple degrees of freedom

To describe a system with multiple degrees of freedom, the finite element form has previously been established. It is repeated here:

$$\boldsymbol{K}\boldsymbol{x} + \boldsymbol{M}\ddot{\boldsymbol{x}} = \boldsymbol{f^I} \tag{14}$$

To find the eigenfrequencies of the system a solution on the form $\boldsymbol{x} = \phi e^{i\lambda t}$ is assumed and free vibrations are considered, i.e. $\boldsymbol{f^I} = \boldsymbol{0}$. By differencing and insertion in equation (14) the following generalized eigenvalue problem is obtained:

$$(\boldsymbol{K} - \lambda_i^2 \boldsymbol{M})\phi_i = \boldsymbol{0} \qquad i = 1, 2, 3...ndof \tag{15}$$

where λ is an eigenvalue and ϕ is an eigenvector. The two create an eigenpair. The number of solutions equation (15) has is the same as the *number of degrees of*

freedom (ndof) without prescribed displacements. Φ is a matrix which holds all the eigenvectors. It can be shown that the eigenmodes are both mass and stiffness orthogonal.

The amplitude of the eigenvectors can not be determined from equation (15), therefore they are normalized to the mass matrix, so that $\Phi^T \boldsymbol{M} \Phi = \boldsymbol{I}$ is fulfilled.
There are several ways to include viscous damping. For example, by rayleigh damping, which is a combination of mass and stiffness, or as a loss factor, which is stiffness dependent. Due to its dependency of for example material, boundary conditions, geometry of the structure and loading situation, damping is usually included based on experience and experimental results. Viscous damping is introduced in equation (14) by a matrix $\boldsymbol{C}$, as:

$$\boldsymbol{K}\boldsymbol{x} + \boldsymbol{C}\dot{\boldsymbol{x}} + \boldsymbol{M}\ddot{\boldsymbol{x}} = \boldsymbol{f^I} \tag{16}$$

Assuming a solution on the form $\boldsymbol{x}(t) = \boldsymbol{u}e^{i\omega t}$, gives velocity $\dot{\boldsymbol{x}}(t) = i\omega \boldsymbol{u}e^{i\omega t}$ and acceleration $\ddot{\boldsymbol{x}}(t) = -\omega^2 \boldsymbol{u}e^{i\omega t}$. It is then possible to go from $\boldsymbol{u}$ to velocity $\boldsymbol{v}$ and acceleration $\boldsymbol{a}$ with a factor of $i\omega$ and $-\omega^2$ respectively. Insertion in equation (16) and setting $\boldsymbol{f^I} = \boldsymbol{f}e^{i\omega t}$ gives:

$$(\boldsymbol{K} + i\omega \boldsymbol{C} - \omega^2 \boldsymbol{M})\boldsymbol{u}e^{i\omega t} = \boldsymbol{f}e^{i\omega t}$$

Here, damping is applied as a loss factor η. As wood and elastomer possess different damping properties this is implemented on element level as follows:

$$\boldsymbol{C} = \frac{1}{\omega}\left[\underset{e\in W}{\mathbb{A}} \eta^w \boldsymbol{k_e^w} + \underset{e\in EL}{\mathbb{A}} \eta^{el} \boldsymbol{k_e^{el}}\right]$$

The governing equations can then be formulated:

$$\begin{gathered} \boldsymbol{D}\boldsymbol{u} = \boldsymbol{f} \\ \boldsymbol{D} = (\boldsymbol{K} + i\omega \boldsymbol{C} - \omega^2 \boldsymbol{M}) \\ \boldsymbol{a} = -\omega^2 \boldsymbol{u} \end{gathered} \tag{17}$$

2.3.4 Modal truncation

Solving the global equation of motion to obtain $\boldsymbol{u}$ quickly becomes computational expensive as the frequency span grows large as it needs to be solved for each frequency evaluation point. A more efficient way is to use modal truncation, where the eigenmodes is used as global shape function, to express the displacements. Multiplying each modes with a scalar value q_u, $\boldsymbol{u}$ can be written as a weighted sum:

$$\boldsymbol{u} = \sum_{i=1}^{ndof} \boldsymbol{\phi}_i q_{u,i} \tag{18}$$

q_u determines the influence of each mode in the displacement vector. As we are interested in evaluating $\boldsymbol{u}$ at relativity low frequencies, the influence of higher modes is often neglectible. Therefore, $\boldsymbol{u}$ may be approximated as:

$$\boldsymbol{u} \approx \sum_{i=1}^{m} \boldsymbol{\phi}_i q_{u,i} = \boldsymbol{\Phi}\boldsymbol{q}_u \tag{19}$$

where m is the number of modes included. m will be chosen so that $m << ndof$. Insertion of this in equation (17) and premultiplying with $\boldsymbol{\Phi}^T$ gives:

$$\boldsymbol{\Phi}^T \boldsymbol{D} \boldsymbol{\Phi} \boldsymbol{q}_u = \boldsymbol{\Phi}^T \boldsymbol{f}$$

where $\boldsymbol{D_r} = \boldsymbol{\Phi}^T \boldsymbol{D} \boldsymbol{\Phi}$ is treated as a diagonal matrix (for higher damping ratios, off diagonal terms may need to be considered), so that solving this is reduced to m independent single degree of freedom system. If inserted back in equation (19), the following equations are obtained:

$$\boldsymbol{u} \approx \boldsymbol{\Phi}(\boldsymbol{D_r^{-1}}(\boldsymbol{\Phi}^T \boldsymbol{f}))$$
$$\boldsymbol{a} \approx -\omega^2 \boldsymbol{\Phi}(\boldsymbol{D_r^{-1}}(\boldsymbol{\Phi}^T \boldsymbol{f}))$$

This reduces computational time as the larger $ndof \times ndof$ system do not have to be solved for each frequency evaluation point. Instead an eigenvalue problem is solved and the eigenvectors is reused for the whole frequency span.

2.3.5 Frequency Response Function

To measure the response in frequency domain, several different possibilities exist for example compliance, mobility and accelerance, which is based on displacement, velocity and acceleration. These evaluations measures will not be treated further in this thesis, as interest lies in optimizing the structure and an expression that serve this purpose is sought. When solving the global equilibrium equation (17) for a specific frequency, the acceleration vector $\boldsymbol{a} \in \mathbb{C}^{ndof \times 1}$ can be obtained. To use MMA to solve the optimization problem a real valued scalar is needed. This can be obtained by using the conjugate transpose (Hermitian),

$$\boldsymbol{a}^H \boldsymbol{a}$$

so that each individual complex number in $\boldsymbol{a}$ is multiplied with its complex conjugate which will lead to that the squared length is obtained. This means that each dof is evaluated by its maximum value during a loading cycle. As all dofs in the acceleration vector may not be of interest to evaluate, a matrix $\boldsymbol{R}$ is defined to sort out the dofs that is of interest. Function g is then defined by taking the square root of the expression.

$$g = \sqrt{\boldsymbol{a}^H \boldsymbol{R} \boldsymbol{a}}$$

This is the function that will be used when calculating the objective function g_o, to be defined in Section 3.2.

3 Optimization procedure

To optimize the elastomer layer, we start by implementing the design variables in the global equlibrium equation. Then, the objective function will be establish, which describe the vibrational response of a CLT panel. This is the function we intend to minimize. The interest lies in optimizing the elastomer layer and since the elastomer is favorable for the vibrational response of the panel, a function that constrains the volume of the elastomer is established. When removing, adding and reallocating material, the stiffness of the panel is changed. This is one of the mechanisms of reducing vibrational response. However, since the panel needs to be able to carry static loads a constraint function describing the static stiffness is also established.

3.1 Implementation of design variables

The design variables are implemented on element level, such that each design variable control the behavior of an element in the elastomer layer. As the design variables z are filtered, they are implemented with the variable κ where $\kappa = \kappa(\tilde{\kappa}(\boldsymbol{z}))$. The global $\boldsymbol{D}$ matrix from equation (17) is modified to be assembled as:

$$\boldsymbol{D} = \underbrace{\underset{e\in W}{\mathbb{A}} \boldsymbol{k_e^w} + \underset{e\in EL}{\mathbb{A}} ((\kappa_e)^p + (\kappa_e)^r \eta^{el} i)\boldsymbol{k_e^{el}}}_{\boldsymbol{K}+i\omega\boldsymbol{C}} - \omega^2 \left(\underbrace{\underset{e\in W}{\mathbb{A}} \boldsymbol{m_e^w} + \underset{e\in EL}{\mathbb{A}} (\kappa_e)^q \boldsymbol{m_e^{el}}}_{\boldsymbol{M}} \right) \tag{20}$$

The design variables are then only implemented on elements belonging to the elastomer layer.

3.2 Optimization formulation

To formulate the optimization problem, the response function g presented in Section 2.3.5 is stated here:

$$g = \sqrt{\boldsymbol{a^H R a}}$$

Function g is used to evaluate the response for a specific frequency and load case. As we are interested in optimizing the panels with respect to the vibrational response for a frequency span and not just at a specific frequency, g is evaluated at discrete frequency points over a span and then summed. These discrete points belong to the set Ω_f. It may also be of interest to make sure that we do not just optimize the panels for a single load case, as this may result in that the final design perform well for that load but poorly for other load cases. This aspect is considered by evaluating g for a few representable load cases. These load cases are collected in the set F. It might also be of interest to specifically target the response of the frequency where the response is highest, this requires an approximation of that value. A common method to obtain such an approximation is to use a p-norm, this has been used in for instance (Le et al. 2010), (Holmberg et al. 2013) and has been adopted here. The objective function g_o that is to be minimized, can then be presented:

$$g_o = \left[\sum_{j\in\Omega_f} \left[\sum_{k\in F} g_{jk} \right]^{p^n} \right]^{1/p^n} \tag{21}$$

where g_{jk} is g evaluated at frequency j, for the load case k, and where p^n is a value, which can be chosen so that g_o approximates the response of the frequency that yield the highest response in the frequency span. As it is also of interest to limit the displacement of a static loading situation the following constraint has been used:

$$\frac{\boldsymbol{u}_s^T \boldsymbol{u}_s}{c_u} - 1 \leqslant 0$$

where $\boldsymbol{u_s}$ is the displacements due to static loading, obtained by solving the equilibrium equation $\boldsymbol{K u_s} = \boldsymbol{f_s}$ and c_u is the limit for the displacements. As the elastomer is a material suitable for reducing vibrations, it is not certain that the response is reducible by removing material and therefore a volume constraint is also formulated according to equation (22).

$$\frac{V}{V_o \cdot V_{max}} - 1 \leqslant 0 \qquad\qquad 0 < V_{max} \leqslant 1 \tag{22}$$

Where $V = V(\boldsymbol{\kappa}) = \sum_{e=1}^{ndv} \kappa_e v_e$, ndv is the number of design variables, v_e is the volume of element e. V is then the total volume of elastomer and V_{max} is the fraction of the total volume allowed. V_o is the volume of a filled layer ($V_o = \sum_{e=1}^{ndv} v_e$).
The optimization problem $\mathbb{P}$ can then be formulated as:

$$\mathbb{P} \begin{cases} \min \quad g_o \\ \text{subject to} \quad \begin{cases} \frac{V}{V_o \cdot V_{\max}} - 1 \leq 0 \\ 0 \leq z_i \leq 1, \quad i = 1, 2, \ldots, ndv \\ \boldsymbol{D a} = \boldsymbol{f}, \quad \boldsymbol{f} \in F \\ \frac{\boldsymbol{u}_s^T \boldsymbol{u}_s}{c_u} - 1 \leq 0, \quad \boldsymbol{K u}_s = \boldsymbol{f}_s \end{cases} \end{cases}$$

3.3 Sensitivity analysis

Sensitivity analysis is performed to find the partial derivatives of the objective function and its constraints with respect to each design variable which is used to solve the optimization problem $\mathbb{P}$. Starting with the objective function we have from equation (21):

$$\frac{\partial g_0}{\partial \kappa_e} = \frac{1}{p^n} \left[\sum_{j \in \Omega_f} \left[\sum_{k \in F} g_{jk} \right]^{p^n} \right]^{1/p^n - 1} \sum_{j \in \Omega_f} \left(p^n \left[\sum_{k \in F} g_{jk} \right]^{p^n - 1} \sum_{k \in F} \frac{\partial g_{jk}}{\partial \kappa_e} \right)$$

To find the partial derivatives of g, the expression $\boldsymbol{a}^H \boldsymbol{R a}$ is differentiated.

$$\frac{\partial}{\partial \kappa_e} (\boldsymbol{a}^H \boldsymbol{R a}) = \frac{\partial \boldsymbol{a}^H}{\partial \kappa_e} \boldsymbol{R a} + \boldsymbol{a R} \frac{\partial \boldsymbol{a}}{\partial \kappa_e} \tag{23}$$

The right hand side of (23) holds two complex valued scalars, which are each others complex conjugate. They can therefore be treated as one term by taking the real part of the last term and multiplying by 2:

$$\frac{\partial}{\partial \kappa_e} (\boldsymbol{a}^H \boldsymbol{R a}) = \mathrm{Re} \left[2 \boldsymbol{a}^H \boldsymbol{R} \frac{\partial \boldsymbol{a}^H}{\partial \kappa_e} \right]$$

The term $\frac{\partial \boldsymbol{a}}{\partial \kappa_e}$ is not easily found analytically, and a numerical solution would be to computational expensive. Therefore, the adjoint method is used to eliminate the term.

By premultiplying the differentiated equilibrium with an adjoint vector $\boldsymbol{\Lambda}^T$, where it is assumed that the equilibrium equation is fulfilled, and noting that the external force vector is independent of the design variables, one obtain:

$$\frac{\partial}{\partial \kappa_e}(\boldsymbol{a}^H \boldsymbol{R} \boldsymbol{a}) = \mathrm{Re}\left[2\boldsymbol{a}^H \boldsymbol{R}\frac{\partial \boldsymbol{a}^H}{\partial \kappa_e} + \boldsymbol{\Lambda}^T(\frac{\partial \boldsymbol{D}}{\partial \kappa_e}\boldsymbol{a} + \boldsymbol{D}\frac{\partial \boldsymbol{a}}{\partial \kappa_e})\right]$$
$$\frac{\partial}{\partial \kappa_e}(\boldsymbol{a}^H \boldsymbol{R} \boldsymbol{a}) = \mathrm{Re}\left[\boldsymbol{\Lambda}^T\frac{\partial \boldsymbol{D}}{\partial \kappa_e}\boldsymbol{a} + (2\boldsymbol{a}^H \boldsymbol{R} + \boldsymbol{\Lambda}^T \boldsymbol{D})\frac{\partial \boldsymbol{a}}{\partial \kappa_e}\right]$$

where $\boldsymbol{\Lambda}$ is obtained by solving

$$\boldsymbol{D}\boldsymbol{\Lambda} = -2\boldsymbol{R}\bar{\boldsymbol{a}} \tag{24}$$

where the over-bar denotes the complex conjugate. Furthermore, we note that $\boldsymbol{a} = -\omega^2\boldsymbol{u}$, where $\boldsymbol{u}$ is obtained by solving the equilibrium equation (17). Then, the partial derivatives of g is given by

$$\frac{\partial g}{\partial \kappa_e} = \frac{1}{\sqrt{\boldsymbol{a}^H \boldsymbol{R} \boldsymbol{a}}}\mathrm{Re}\left[\boldsymbol{\Lambda}^T\frac{\partial \boldsymbol{D}}{\partial \kappa_e}\boldsymbol{a}\right] \tag{25}$$

where, from equation (20), we have:

$$\frac{\partial \boldsymbol{D}}{\partial \kappa_e} = (p\kappa_e^{p-1} + r\kappa_e^{r-1}\eta^{el}i)\boldsymbol{k}_e^{el} - \omega^2 q\kappa_e^{q-1}\boldsymbol{m}_e^{el}$$

To compute the sensitivities of the objective function there is therefore two large equation systems to solve, equation (24) and (17), and these has to be solved for each evaluation of g. However, the same factorization of $\boldsymbol{D}$ can be used to solve for both $\boldsymbol{\Lambda}$ and $\boldsymbol{a}$. This requires a factorization of $\boldsymbol{D}$ each frequency step, a faster way is to use modal truncation, which has been described above for computing $\boldsymbol{a}$. This procedure will be described in the next section for computing $\boldsymbol{\Lambda}$.
As we have $g_o = g_o(\boldsymbol{\kappa}(\bar{\boldsymbol{\kappa}}(\boldsymbol{z})))$, we utilize (8) and (9) to obtain:

$$\frac{\partial \tilde{\boldsymbol{\kappa}}}{\partial \boldsymbol{z}} = \boldsymbol{A}^F = A^F_{jk}$$

$$\frac{\mathrm{dH}}{\mathrm{d}\bar{\kappa_i}} = \frac{\beta \mathrm{sech}^2\beta(\bar{\kappa_i} - \eta)}{\tanh\beta\eta + \tanh\beta(1-\eta)}$$

So that the final partial derivative of the objective function with respect to design variable z_j can be obtained by:

$$\frac{\partial g_o}{\partial z_j} = \sum_{k=1}^{ndv} A^F_{jk}(\frac{\mathrm{dH}}{\mathrm{d}\bar{\kappa_k}}\frac{\partial g_o}{\partial \kappa_k})$$

where ndv is the number of design variables. For the volume constraint we have $\frac{\partial V}{\partial \kappa_e} = v_e$ and as before $V = V(\boldsymbol{\kappa}(\bar{\boldsymbol{\kappa}}(\boldsymbol{z})))$. As the displacement constraint is similar to the response function, the derivation of the sensitivities will also be so and is therefore not presented here.

3.4 Truncation of sensitivities

It has previously been described how the system can be reduced by using modal truncation to solve the global equilibrium equation. As $\boldsymbol{D}$ still needs to be factorized to solve for $\boldsymbol{\Lambda}$, the computational gain is neglectible. Therefore, $\boldsymbol{\Lambda}$ is approximated by using the same procedure as was used for approximating $\boldsymbol{u}$, i.e.:

$$\boldsymbol{\Lambda} \approx \sum_{i=1}^{m} \phi_i q_{\Lambda,i} = \boldsymbol{\Phi} \boldsymbol{q}_{\Lambda} \tag{26}$$

Insertion of eq. (26) in eq. (24) and premultiply with $\boldsymbol{\Phi}^T$ gives

$$\begin{aligned} \boldsymbol{D}_r \boldsymbol{q}_{\Lambda} &= -2\boldsymbol{\Phi}^T \boldsymbol{R}\bar{\boldsymbol{a}} \\ \boldsymbol{D}_r &= \boldsymbol{\Phi}^T \boldsymbol{D} \boldsymbol{\Phi} \end{aligned} \tag{27}$$

By inserting eq. (27) back into eq. (26) an approximated way to compute Λ is obtained:

$$\boldsymbol{\Lambda} \approx -2\boldsymbol{\Phi}(\boldsymbol{D}_{\boldsymbol{r}}^{-\mathbf{1}}(\boldsymbol{\Phi}^T \boldsymbol{R}\bar{\boldsymbol{a}})) \tag{28}$$

A similar approximation is used in (Dahlberg et al. 2023) for buckling constraint where it leads to the same solution as for solving the full system. In appendix D, the accuracy of this approximation has been evaluated.

4 Numerical examples

Three examples of optimized designs where the optimization problem $\mathbb{P}$ is solved are presented, one 3 layer panel and two 5 layer panels. The panels are 4×3 m with each layer of wood being 20 mm. The optimized designs have been modelled with a 2 mm elastomer layer where the volume constraint has been set to have a total of 50% or less material in that layer, the rest is then voids. The static displacement constraint is subject to an even distributed load, from where the displacement at the center of the panel is prescribed to a 10% increase from the starting design. The starting design is a completely filled elastomer layer.

To evaluate the dynamic response, the loads are applied on a symmetry quarter of the panels, and is applied as four point loads. Where each point load is evaluated individually. This is to obtain robustness, as explained further in Appendix C. The applied loads are shown in Figure 8.

The penalization parameters, explained in Appendix B, are set to $p = 1$, $q = 1$ and $r = 2$. The frequency step size, which is the length between the discrete frequency evaluation points is 0.1 Hz when optimizing, and 0.05 Hz when evaluating the optimized designs, the reasoning behind this is presented in Appendix A. The dofs that has been included in the objective function (sorted out by the matrix $\boldsymbol{R}$) is located at the top surface of the panels, with direction orthogonal to the surface. This is the same dofs that has been used when the result has been evaluated. Heaviside parameter β starts at a 10^{-6} and starts update by 1 at the 15th iteration and is then increased with 1 every 5th iteration. Approximately 200 iterations were needed to reach a fully converged design.

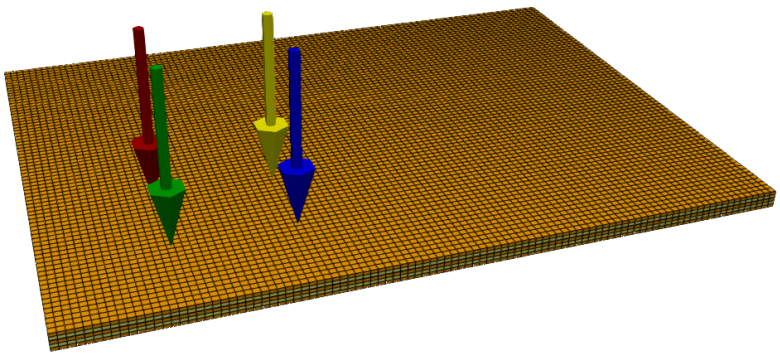

Figure 8: *The load applied to the panels when evaluating the objective function. Each arrow corresponds to a force vector.*

The optimized design has been compared to a corresponding model but with 1 mm uniform elastomer layer. This way the optimized design is compared to a design with the same amount of elastomer but with a different distribution. The designs have

either been evaluated as the function g

$$g = \sqrt{\boldsymbol{a}^H \boldsymbol{R} \boldsymbol{a}}$$

which is the function used when calculating the objective function g_o, or as average acceleration defined as:

$$a_{mean} = \frac{1}{k} \sum_{j=1}^{k} \text{abs}(a_j^R)$$

where a^R is the dofs that is evaluated as described above. To ensure that the design do not only perform well for the load applied during optimization, different load cases has been used when evaluating the designs. The symmetry quarter of the panels has been divided in 5×5 load zones, where traction force is applied and evaluated in each zone. Both functions used to evaluate results has been either summed for all of the external forces vectors or the envelope has been taken by using the response for the load that gives the largest response at each frequency step.

4.1 Material parameters

The wood in the panels has been modelled according to transversal isotropy described in Section 2.1. With material parameters presented in Table 1 where E_L is young's modulus in the fiber direction and E_T is young's modulus transversal to the fiber. G_{LT} is the shear modulus between the fiber direction and the transversal plane. ν_{LT} is Poisson's ratio between the direction of the fiber and the transversal plane when loaded in the direction of the fiber. ν_T is Poisson's ratio in the transversal plane. The density for wood is $\rho^w = 420$ kg/m^3 and for elastomer $\rho^e = 500$ kg/m^3

Table 1: *Material parameters for wood panels*

E_L	E_T	G_{LT}	ν_{LT}	ν_T
11 GPa	370 MPa	690 MPa	0.3	0.4

For the elastomer, an isotropic material model is used, also described in Section 2.1, with a Young's Modulus of 10 MPa and Poisson's ratio $\nu = 0.42$. The loss factor for the elastomer layer is $\eta^{el} = 0.15$ and for wood $\eta^w = 0.012$.

4.2 3 Layer panel

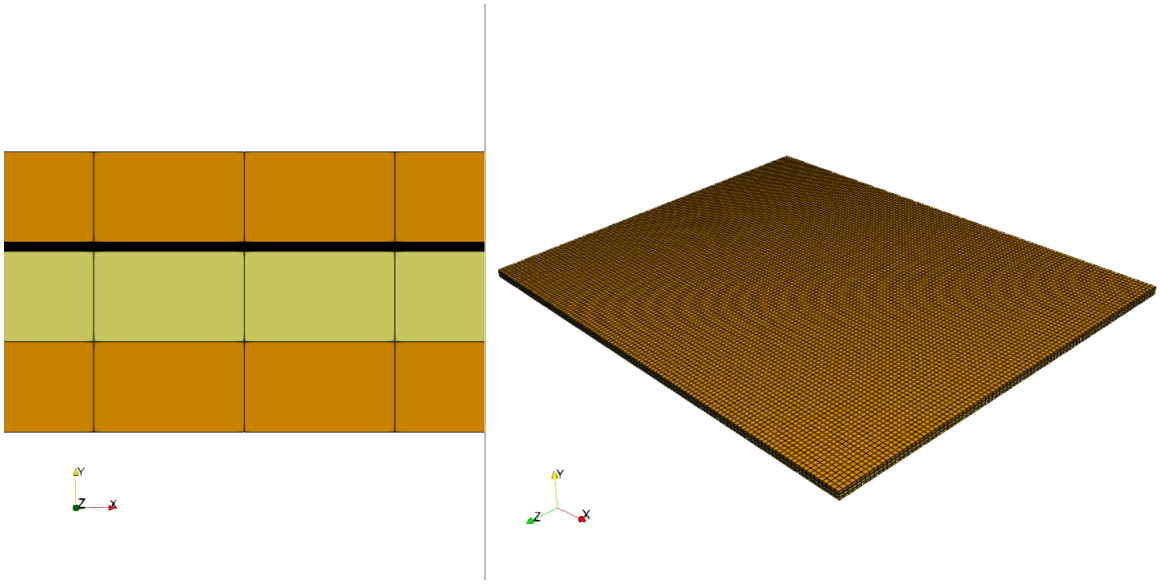

Figure 9: *Discretization of a 3 layer panel. Top and bottom elements has the fiber directed along the x-axis, elements in the middle has the fiber direction along z-axis. Black elements is the elastomer layer. The panel is 4 m in x-direction and 3 m in z-direction.*

A model of a 3 layer panel has been established according to Figure 9 and with the conditions stated at the beginning of this section. The frequency span this panel is optimized for is set to $5 - 80$ Hz, this gives approximately the same number of eigenfrequencies in the span as $5 - 120$ Hz gives for the 5 layer panel. The boundary condition of the static loading is applied at the shorter edges and is applied so that the panel is simply supported.

When evaluating the objective function there are none prescribed displacement dofs. The load applied is described in the beginning of this section. The p-norm value is set to $p^n = 1$ so that all values over the frequency span is given the same weight. Mode $7 - 30$ are included when calculating the objective function, rigid body modes are thereby neglected. When evaluating the design, mode $1 - 50$ are considered, thus, rigid body modes are also included. The element length is 3.33 cm in the x and z direction, respectively.

The design obtained when solving the optimization problem $\mathbb{P}$ from above conditions is presented in Figure **??**.

The response over the frequency span is reduced, shown in Figure 15. As an attempt to understand the optimized designs, the mode shapes have been plotted in Figure 12 and 13 on top of the optimized design, by coloring regions with a transparent color where the displacement of the modes are less than 20% of the maximum value. It can be seen that several of the modes seems to fit the pattern of the design. In Figure 14, each eigenfrequency has been marked with the same color as the corresponding mode in Figure 12 and 13. The mode shapes are presented in Figure 11.

The result analysis indicate that the optimized design performs well even when the frequency span is larger than what is included in the optimization procedure. This can be seen in Table 2, where different frequency spans, and the two evaluation function

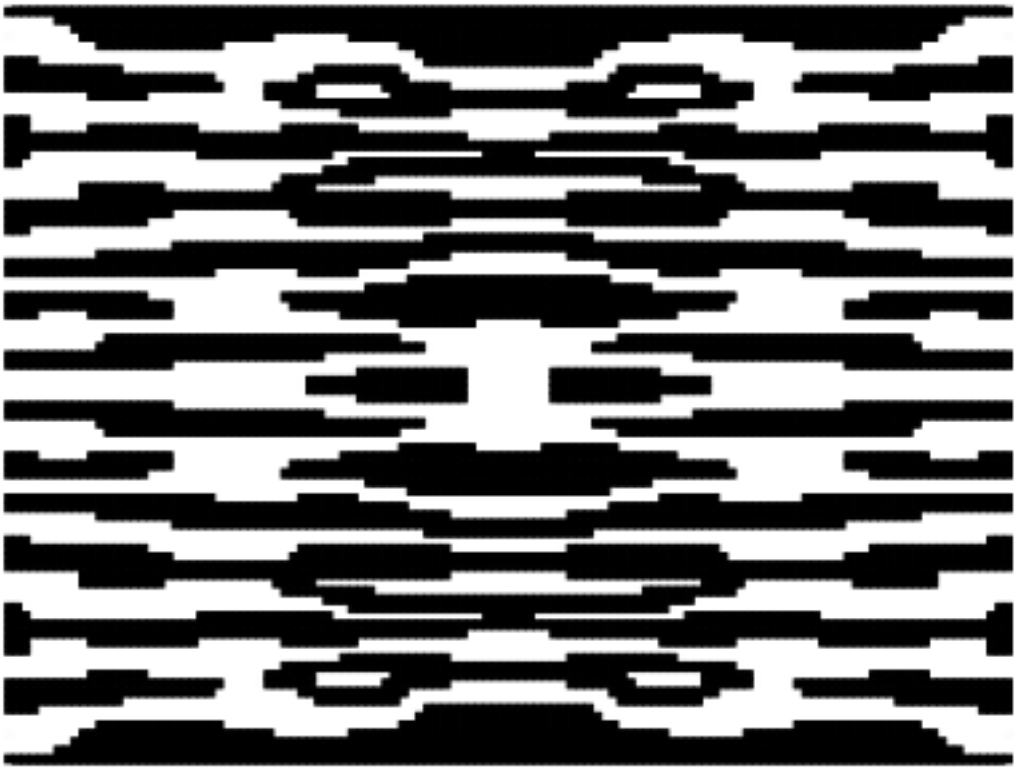

Figure 10: *Optimized design of a 3 layer CLT panel. The figure shows the elastomer layer where black regions are elastomer and white regions are void*

has been compared. The frequency span of $5 - 150$ has been plotted in Figure 16. Where the optimized layer performs better than the uniform layer even outside the frequency span that has been included in the optimization.

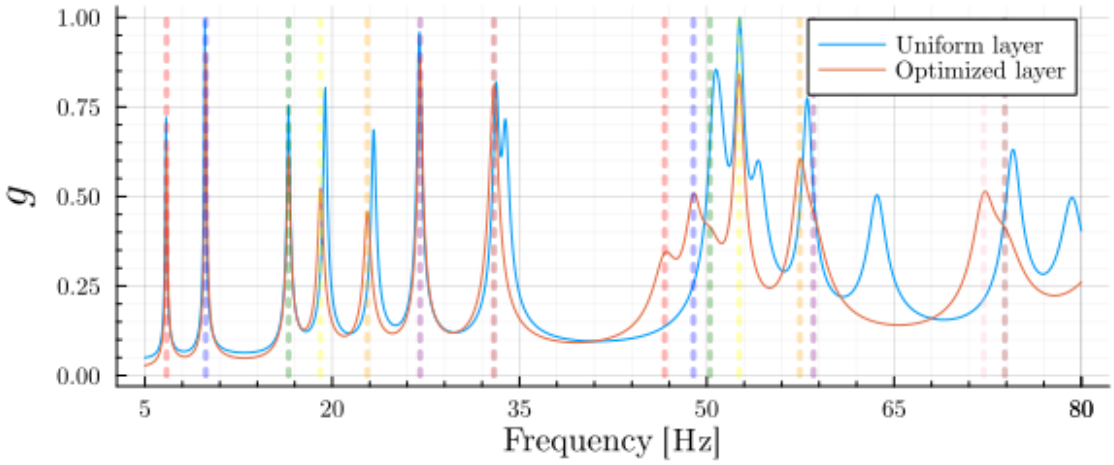

Figure 14: *The colors of the dotted lines corresponds to the color of the modes presented in Figure 12 and 13. In this figure the function g has been used to evaluate the response, the uniform distribution of the elastomer layer is compared to the optimized.*

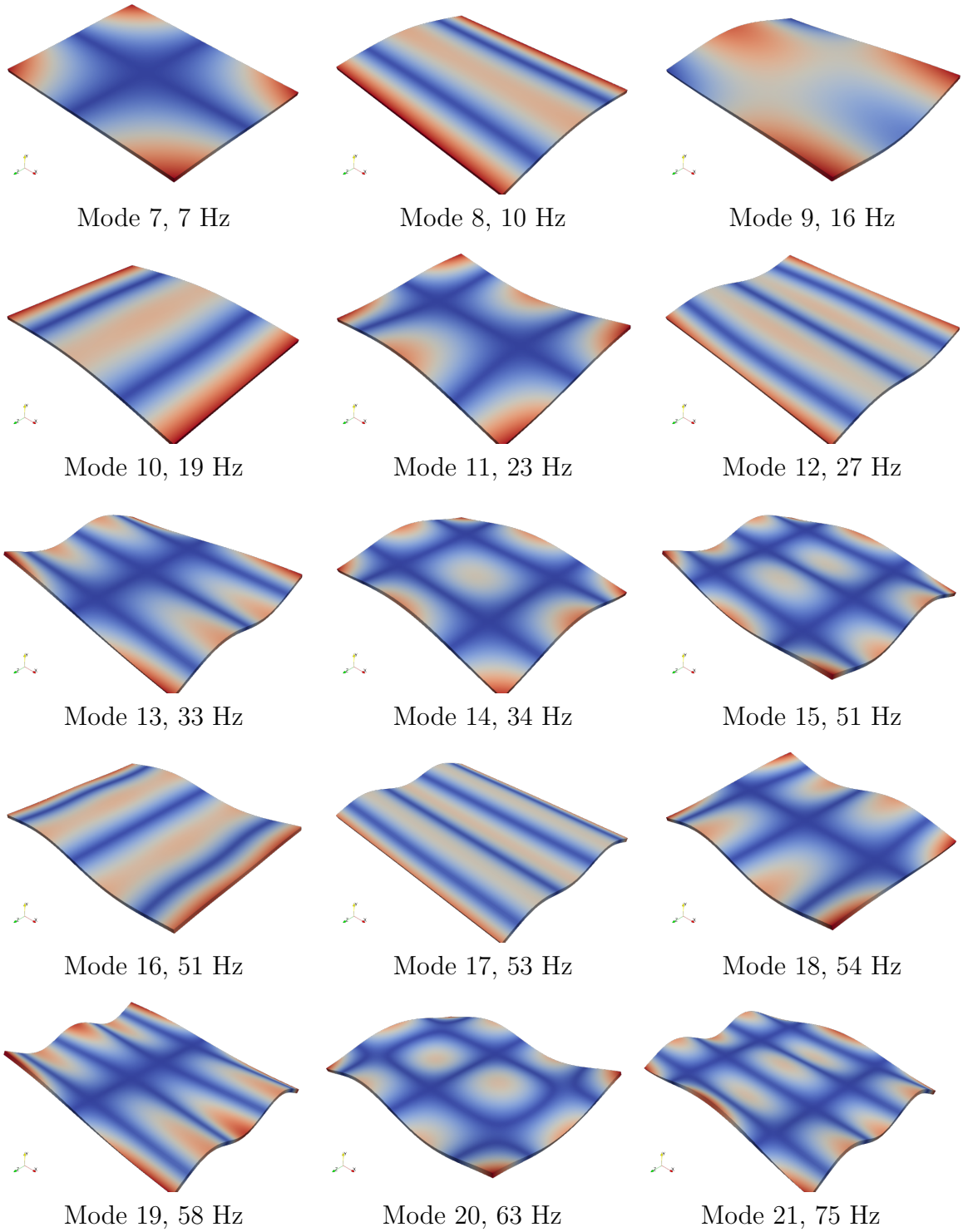

Figure 11: *Mode 7-21 for a 3 layer panel with corresponding eigenfrequency.*

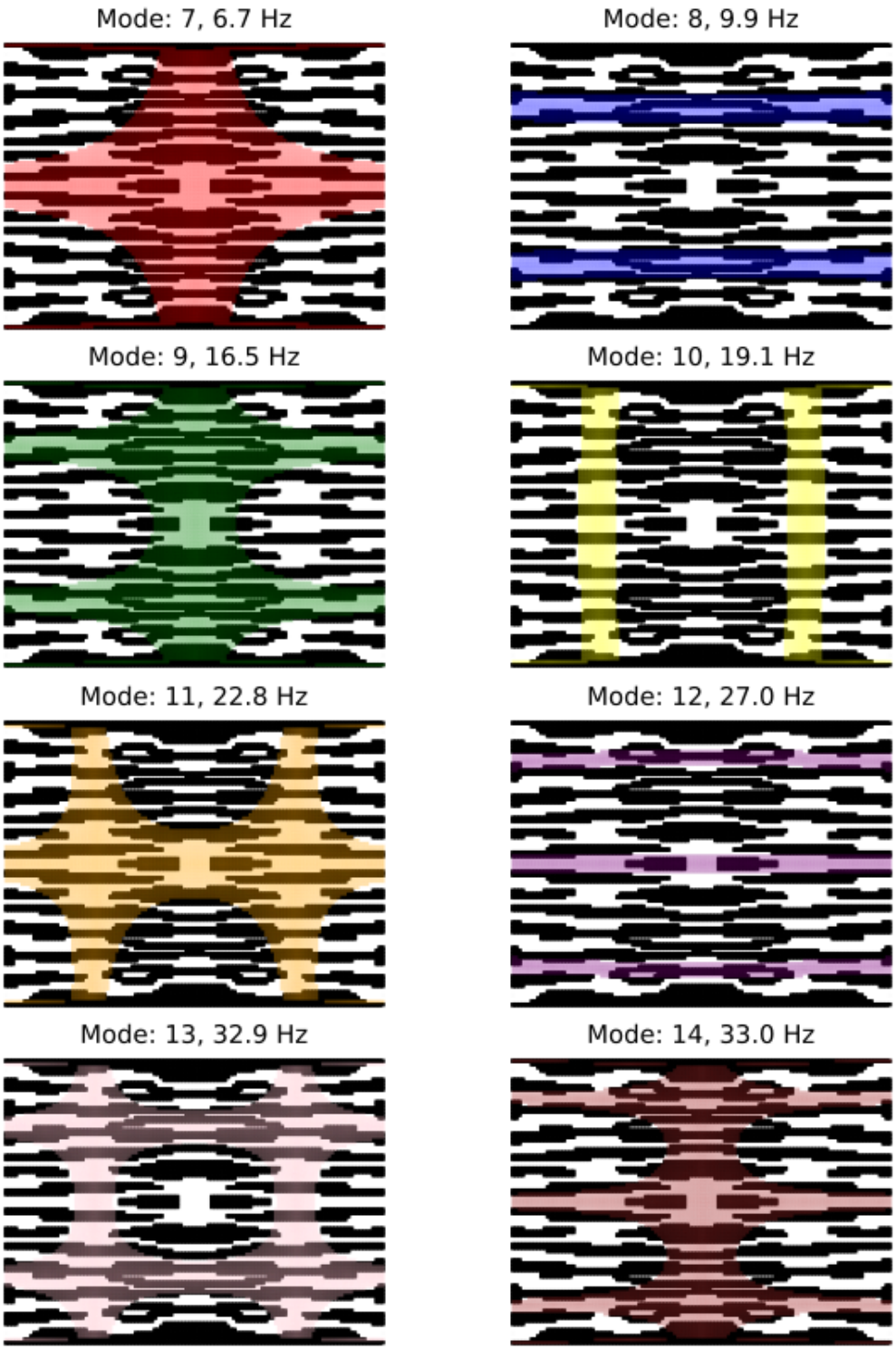

Figure 12: *Optimized design. Regions where the displacement of the respective mode is less than* 20% *of its maximum value is marked with transparent color.*

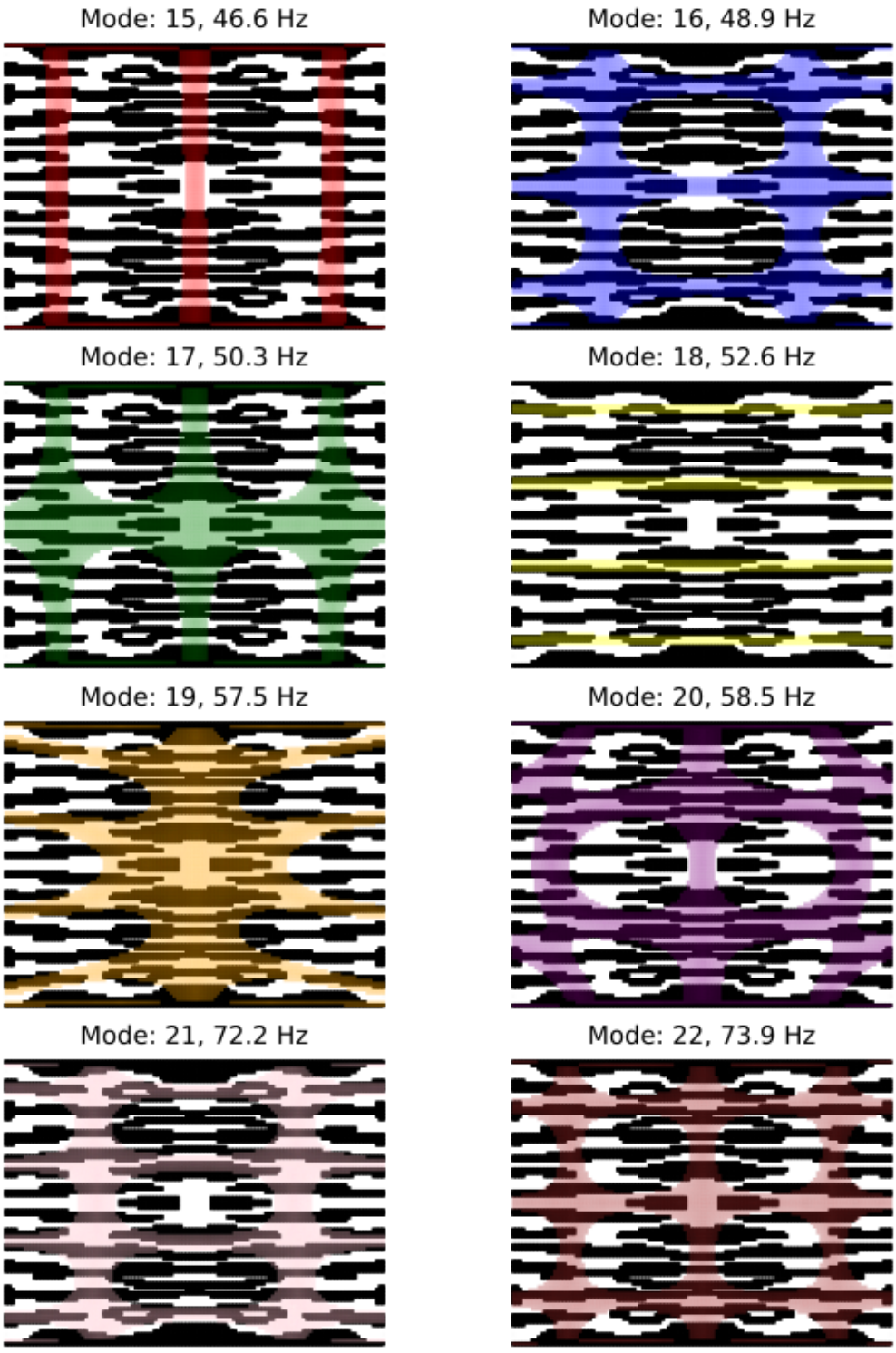

Figure 13: *Optimized design. Regions where the displacement of the respective mode is less than* 20% *of its maximum value is marked with transparent color.*

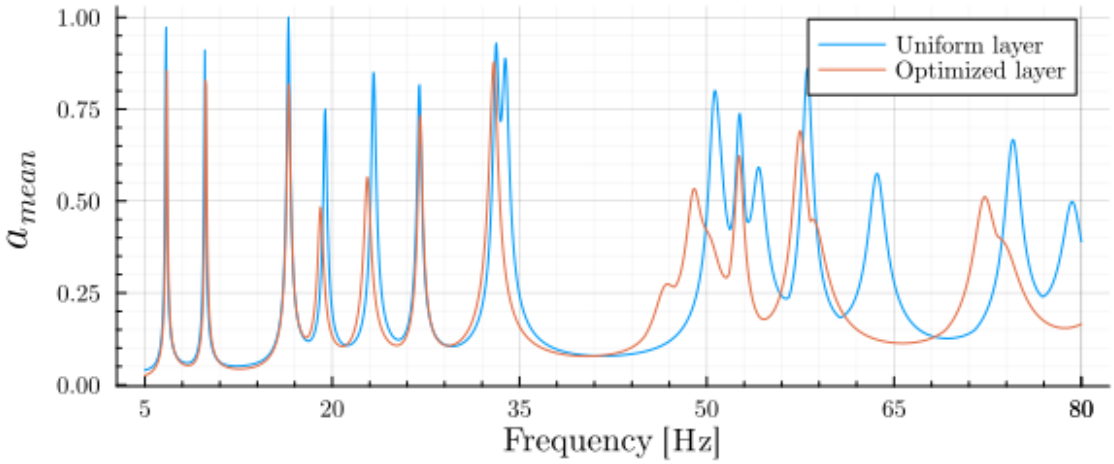

Figure 15: *Optimized elastomer layer compared to uniform distribution. Evaluated by the envelope of a_{mean} for the load which gives largest response at each frequency*

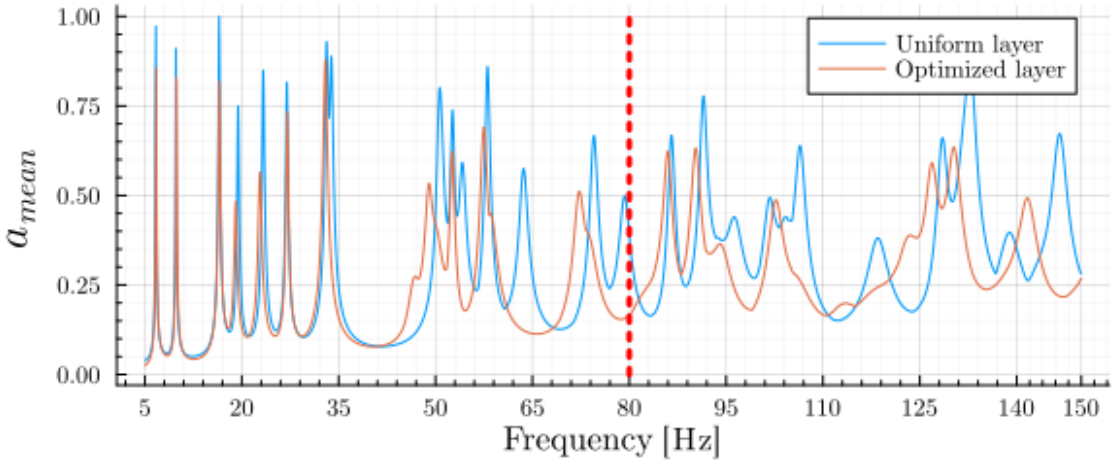

Figure 16: *Envelope of average acceleration for the load which gives largest response at each frequency. Left side of the red line is included in the optimization.*

Table 2: *Sum, RMS and RMQ values over different frequency spans for the optimized panel, evaluated by function g or a_{mean}. The values are normalized to the corresponding values of a uniform distribution of the elastomer.*

Function	Loads evaluated	Frequency span	$\sum$	RMS	RMQ
g	all	5-80 Hz	0.89	0.86	0.84
g	all	5-150 Hz	0.9	0.88	0.86
a_{mean}	all	5-80 Hz	0.9	0.87	0.84
a_{mean}	envelope	5-80 Hz	0.86	0.84	0.83

4.3 5 Layer panel

The optimization problem $\mathbb{P}$ has been solved for two 5 layer panels, the first has been solved without prescribed displacement dofs when calculating the objective function (free-free). The second has been evaluated as a simple supported panel in both directions. The discretization of the panel is shown in Figure 17. The frequency span considered ranges from 5 to 120 Hz. The element size in x and z direction is 4 cm respectively. The p-norm value is set to $p^n = 8$ which means that the of frequencies with larger response is weighted more in the objective function.

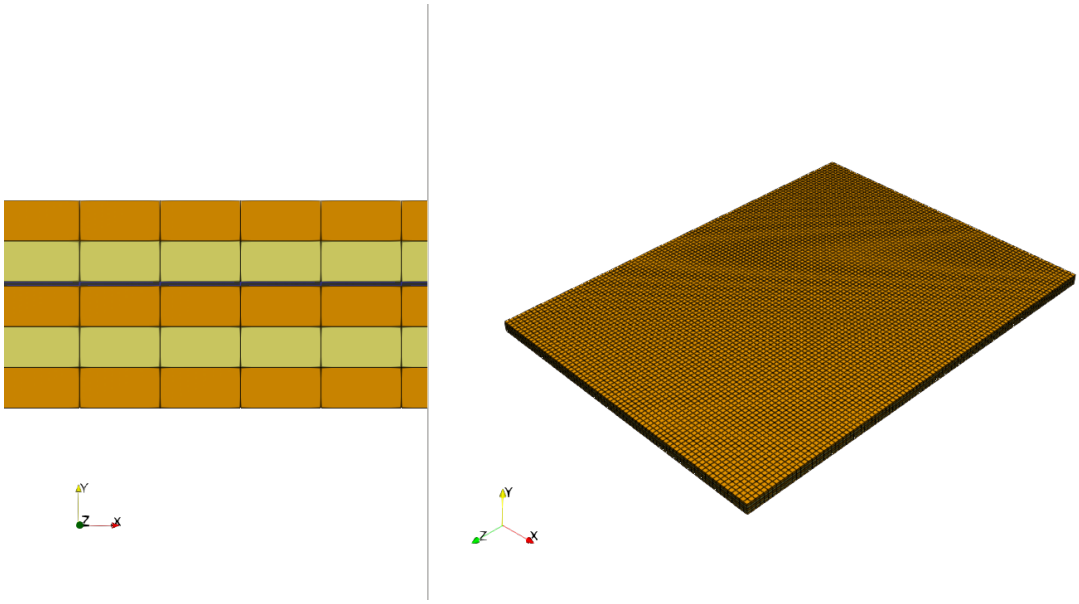

Figure 17: *Discretization of a 5 layer panel. Top, bottom, middle elements has the fiber directed along the x-axis, the two remaining layers (yellow) has the fiber direction along z-axis. Black elements is the elastomer layer. The panel is 3 m in x-direction and 4 m in z-direction.*

4.3.1 Without prescribed displacement boundary conditions

The panel in this section has been optimized without prescribed displacement dofs when calculating the objective function, the 7th to 30th modes are included when using modal analysis to optimize the panel. When evaluating the design, mode $1-60$ is used. The design obtained is presented in Figure 18.

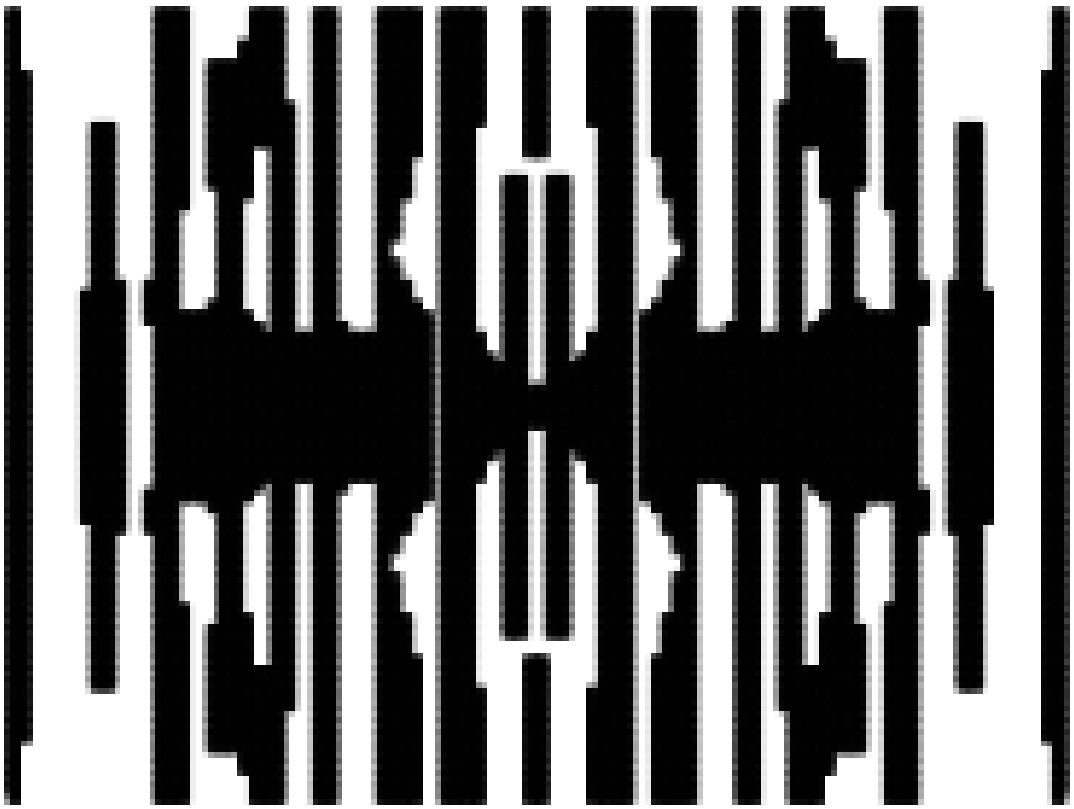

Figure 18: *Optimized design of the elastomer layer in a 5 layer panel without displacement prescribed dofs. The black areas are elastomer and white are void.*

The lines from short edge to short edge could be interpreted as necessary for maintaining the static stiffness, as this would be the load-carrying direction. It is also likely that some of the modes fits the pattern of the design, in the same manner was as shown for the 3 layer panel. The mode shapes of the panel are presented in Figure 19.

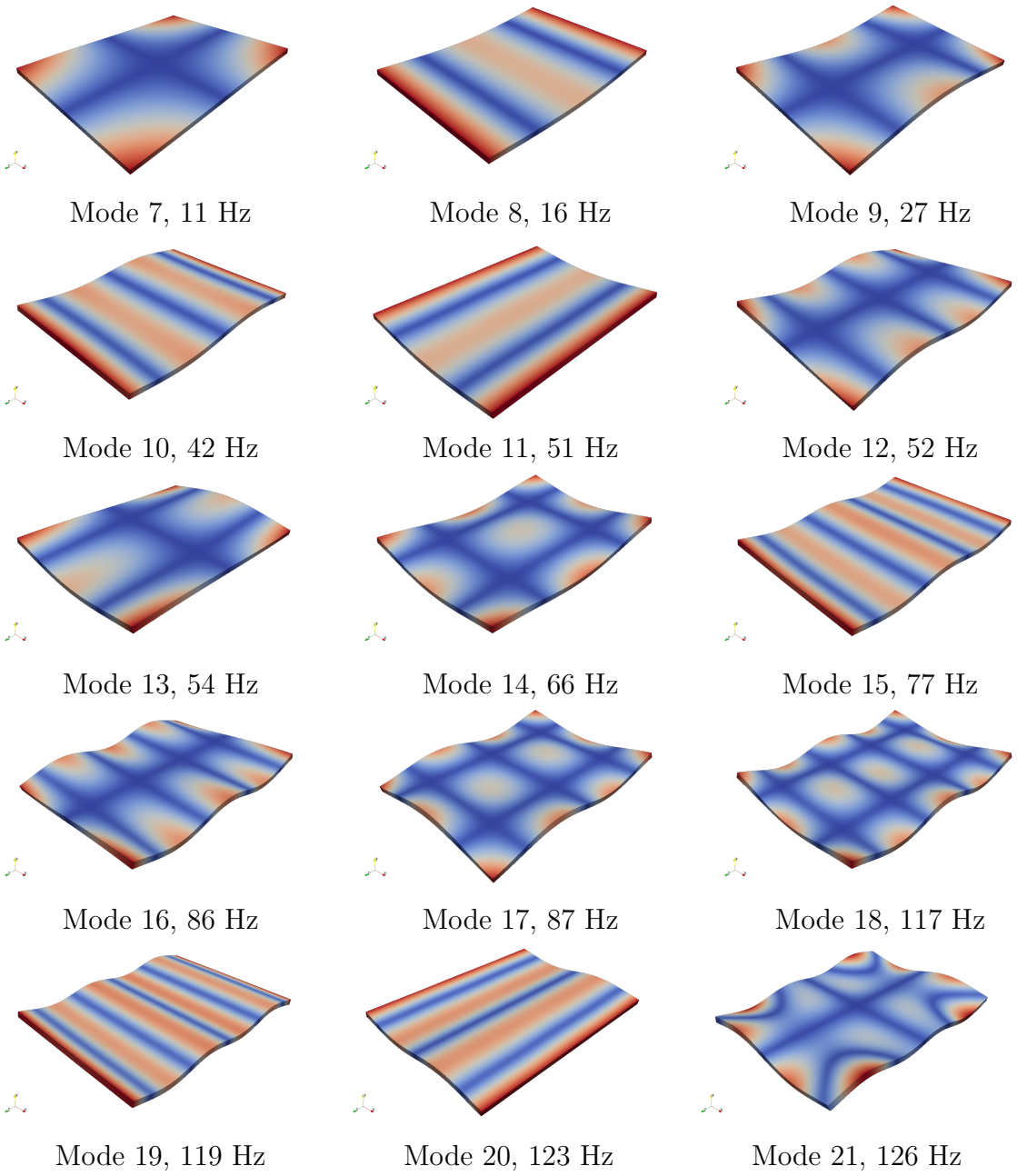

Figure 19: *Mode* $7 - 21$ *with corresponding frequency for the 5 layer panel without displacement prescription.*

In Figure 20 the optimized design is compared to a uniform distribution of the elastomer layer. The function g is used as an evaluation measure as this is the same function used when optimizing the design. It can be seen that the response is reduced for the optimized design, especially is the highest values reduced and this is what is expected when using a p-norm to approximate the highest response over the frequency span.

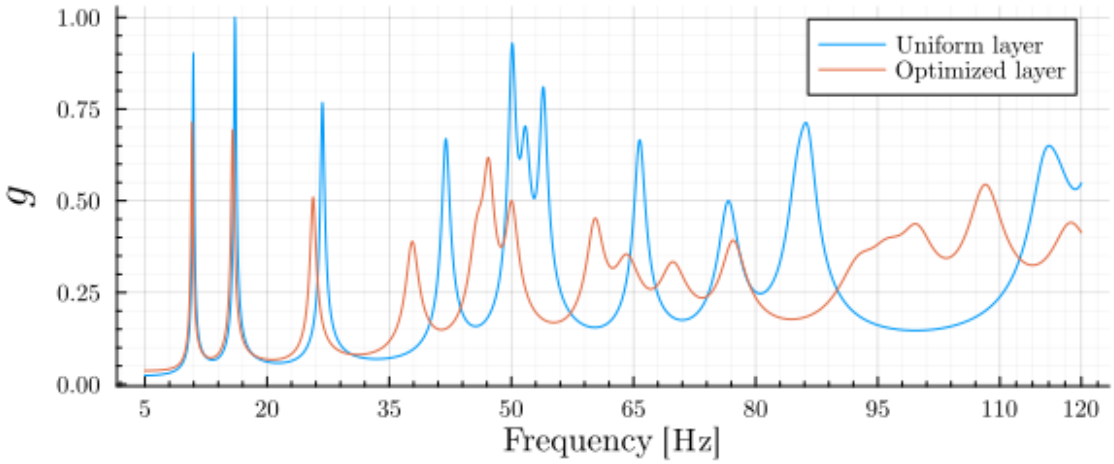

Figure 20: *Optimized distribution compared to uniform distribution. Response is evaluated by the function g.*

When using a_{mean} to evaluate the response, the comparison between optimized and uniform distribution is similar to g. a_{mean} is plotted in Figure 21.

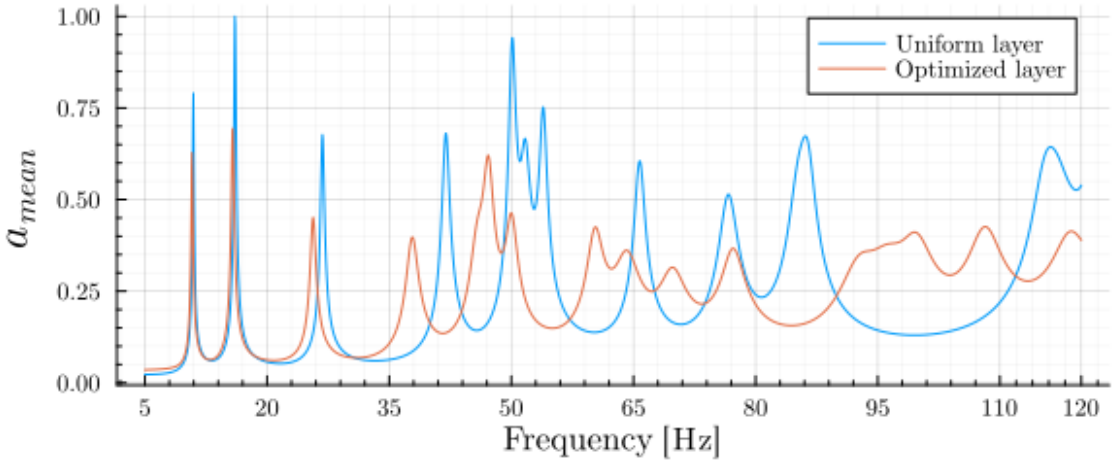

Figure 21: *Optimized distribution compared to uniform distribution. Response is evaluated by the function a_{mean}.*

For this panel the stiffness when applying a point load has been investigated and is presented in Figure 22. The load has been applied and evaluated at the same place. This has been done along a line from the middle of one of the shorter edges towards the center of the panel.

Table 3: *Sum, RMS and RMQ values over different frequency spans for the optimized panel, evaluated by function g or a_{mean}. The values are normalized to the corresponding values of a uniform distribution of the elastomer.*

Function	Loads evaluated	Frequency span	$\sum$	RMS	RMQ
g	all	5-120 Hz	1.03	0.93	0.81
g	all	5-150 Hz	0.96	0.88	0.79
a_{mean}	all	5-120 Hz	1.0	0.89	0.77
a_{mean}	envelope	5-120 Hz	1.06	0.93	0.8

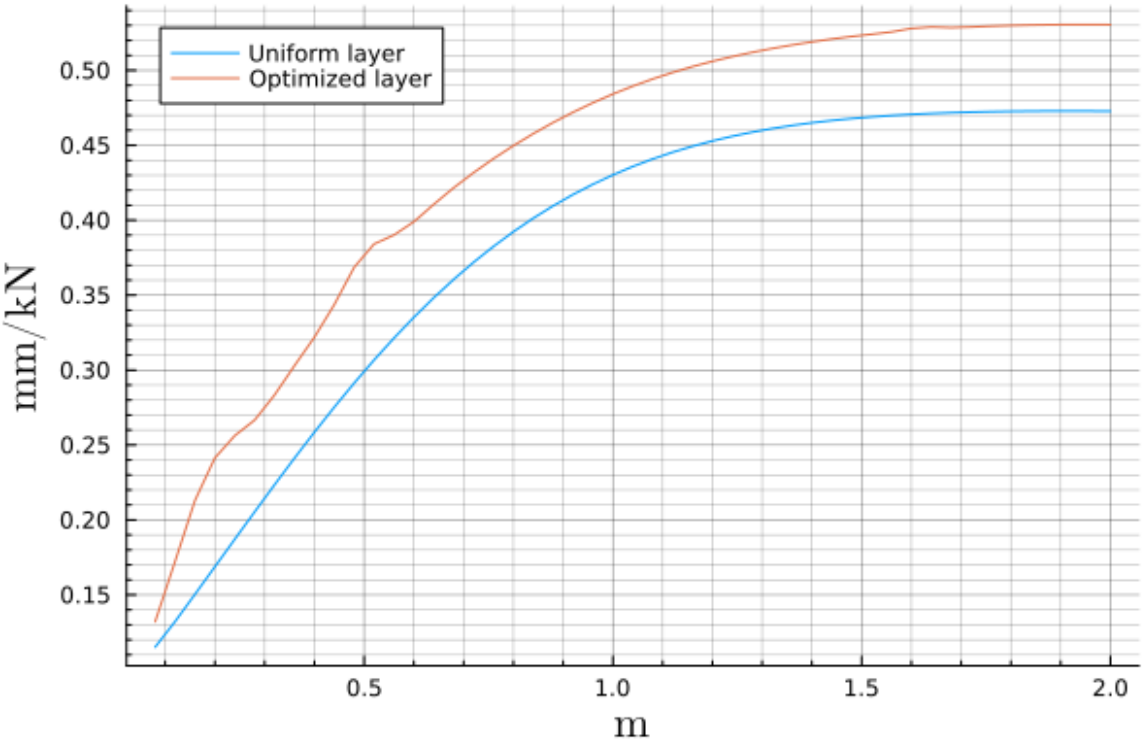

Figure 22: *Static displacement applied and evaluated in the same dof. For all dofs along the centerline in the panels length direction. On the x-axis, distance from the shorter edge is shown.*

The result in table 3 shows that the largest peaks is likely to be reduced more as the RMS and RMQ values are reduced more than the summed values. It can also be noted that the frequency span that might be most reduced is $5 - 150$ Hz. This indicates that the design perform well even for frequencies that is outside the optimized span. A small contribution to this can also be that when making the panel weaker, more eigenfrequencies exist in the frequency span of $5 - 120$Hz for the optimized panel compared to the uniform distribution.

4.3.2 With prescribed displacement boundary conditions

The next design presented is optimized with prescribed displacement dofs around the bottom edge so that the panel is simply supported in both directions. Mode $1 - 20$ has been used when optimizing the panel and $1 - 50$ when evaluating the optimized

design. The design is presented in Figure 23. The mode shapes are presented in Figure 24.

Figure 23: *Optimized design of the elastomer layer in a 5 layer panel without displacement prescribed dofs. The black areas are elastomer and white are voids.*

Table 4: *Sum, RMS and RMQ values over different frequency spans for the optimized panel, evaluated by function g or a_{mean}. The values are normalized to the corresponding values of a uniform distribution of the elastomer.*

Function	Loads evaluated	Frequency span	$\sum$	RMS	RMQ
g	all	5-120 Hz	0.96	0.87	0.77
g	all	5-150 Hz	1.1	1.04	0.95
a_{mean}	all	5-120 Hz	0.97	0.88	0.78
a_{mean}	envelope	5-120 Hz	0.92	0.83	0.73

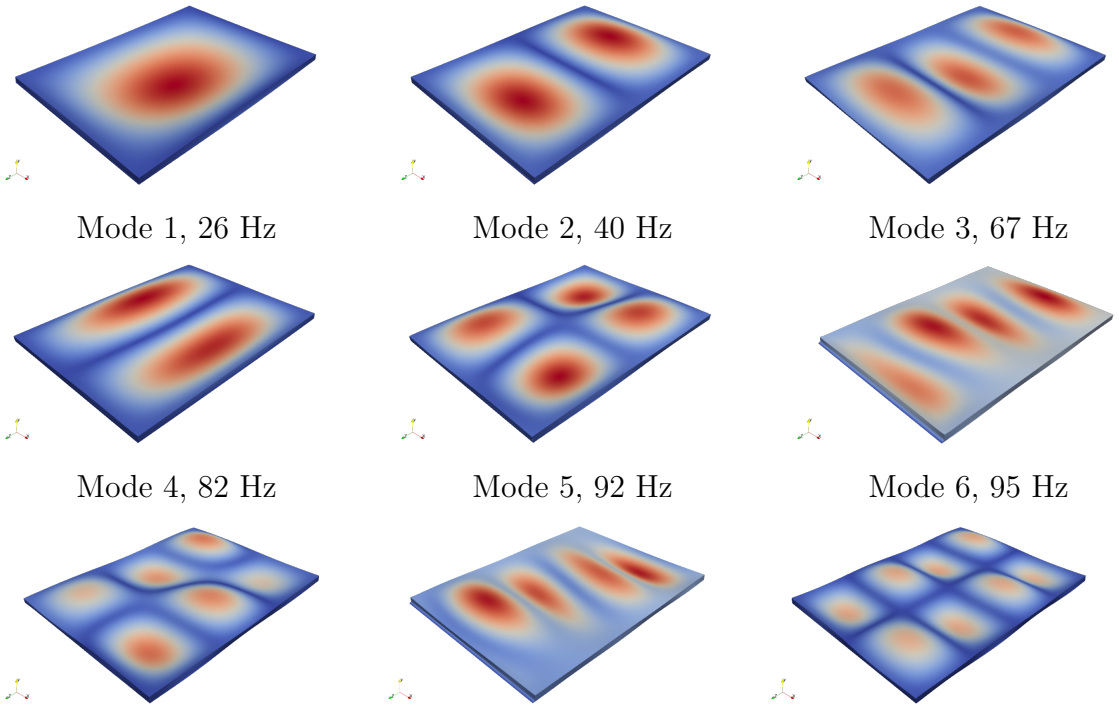

Figure 24: *Mode* $1-9$ *for a 5 layer panel with prescribed displacement at the bottom edges around the panel.*

It can be seen that the peak values is clearly reduced. This is shown in Figure 25 and Table 4. As this panel is modelled with prescribed displacement dofs, the number of eigenfrequencies in the span is lower than previous design.

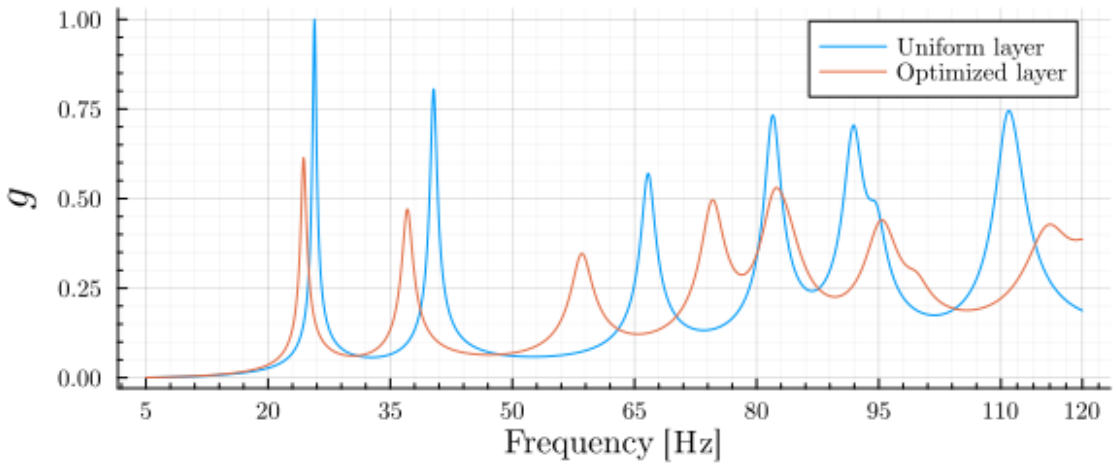

Figure 25: *Optimized design compared to uniform distribution for a 5 layer panel. The panel is simply supported.*

5 Conclusions

The results presented show that it is possible to reduce the response by optimizing for the configuration of the elastomer layer. In the presented examples, by changing the configuration, lead to reduction of vibration in the range of $10 - 20\%$ for RMS values. The potential drawback of this is decrease in static stiffness, and that eigenvalues appear at lower frequencies. This effect could possibly be mitigated by including more design variables, that could for instance involve the wood, switching parts of it to different stiffness or density properties. The physics behind the results is not easily interpreted, as this includes both changes in stiffness and damping in the panels, as well as the connection between the layers above and underneath the elastomer layer. The designs presented is influenced by the mode shapes which is natural as these are fundamental for the dynamic behavior. It may be suspected that a design pattern that fits some modes may also reduce the response of some modes that are not explicitly considered in the optimization procedure, if the node lines in the modes fits the pattern of the design.

To lower the largest response over the frequency span of interest, the use of a p-norm to approximate the largest value in the objective function seems to yield a satisfying result, as the response seems to be reduced more for frequencies with high response. The summed values over the frequency span is reduced more when having an inactive p-norm (3 layer panel) than they are when using a p-norm (5 layer panels), then the RMS values is reduced more.

Modal analysis, and using the fact that each frequency step is independent of each other, which makes it easy to split the computations into different threads, makes it possible to target a large frequency span with reasonable computational time. For the designs presented, solving eigenvalue problem and calculating sensitivities are the most time consuming in the optimization process, where both has required approximately the same computational time.

References

Chopra, A. K. (2020). *Dynamics of structures*. Ed. by William J. Hall. Pearson.

Christensen, P. W. and A. Klarbring (2009). *An Introduction to Structural Optimization*. Springer.

Dahlberg, V., A. Dalklint, M. Spicer, O. Amir and M. Wallin (2023). "Efficient buckling constrained topology optimization using reduced order modeling". In: *Structural and Multidisciplinary Optimization* 66. DOI: https://doi.org/10.1007/s00158-023-03616-7.

Holmberg, E., B. Torstenfelt and A Klarbring (2013). "Stress constrained topology optimization". In: *Struct Multidisc Optim* 48. DOI: https://doi.org/10.1007/s00158-012-0880-7.

Lazarov, B. S. and O. Sigmund (2011). "Filters in topology optimization based on Helmholtz-type differential equations". In: *International Journal for Numerical Methods in Engineering* 86.6, pp. 765–781. DOI: https://doi.org/10.1002/nme.3072. eprint: https://onlinelibrary.wiley.com/doi/pdf/10.1002/nme.3072. URL: https://onlinelibrary.wiley.com/doi/abs/10.1002/nme.3072.

Le, C, J. Norato, T. Bruns, C. Ha and D. Tortorelli (2010). "Stress-based topology optimization for continua". In: *Structural and Multidisciplinary* 41. DOI: https://doi.org/10.1007/s00158-009-0440-y.

Ljunggren, F (2023). "Innovative solutions to improved sound insulation of CLT floors". In: *Developments in the Built Environment* 100117.

Ottosen, N. and H. Petersson (1992). *Introduction to the Finite Element Method*. Pearson.

Ottosen, N. and M. Ristinmaa (2005). *The Mechanics of Constitutive Modeling*. Elsevier.

Pedersen, N. (2000). "Maximation of eigenvalues using topology optimization". In: *Structural and Multidisciplinary Optimization* 20.

Svanberg, K. (1987). "The method of moving asymptotes—a new method for structural optimization". In: *International journal for numerical methods in engineering* 24.2, pp. 359–373.

Wallin, M., N. Ivarsson, O. Amir and D. Tortorelli (2020). "Consistent boundary conditions for PDE filter regularization in topology optimization". In: *Structural and Multidisciplinary Optimization* 62, pp. 1299–1311. DOI: https://doi.org/10.1007/s00158-020-02556-w.

Wang, F., B.S Lazarov and Ole Sigmund (2011). "On projection methods, convergence and robust formulations in topology optimization". In: *Structural and Multidisciplinary Optimization* 43, pp. 767–784. DOI: https://doi.org/10.1007/s00158-010-0602-y.

A Frequency step

As the objective function is evaluated over discrete points across the considered frequency span, the frequency spacing must be chosen carefully. The optimizer finds that an efficient way to minimize the response, is to center the eigenfrequencies between two evaluation points so that the peak value is cut. Therefore, a step size short enough to capture the peak values is needed. To establish how close these evaluation points must be, optimization has been performed between $5 - 20$ Hz, as the peaks tends to be more narrow at lower frequencies. Step lengths of $0.2, 0.15, 0.1, 0.05$ Hz has been used when optimizing, result are presented in Figure 26. Where the orange line is the optimized solution, which has been plotted with a step length, half of what it has been optimized with, so that it can be seen where the peak values have been cut. Even though the first peaks are cut, a frequency step of 0.1 Hz has been used since this is most likely not an issue at higher frequencies since the peaks are then wider and the impact on the optimized designs are expected to be small. To make sure the result presented is not incorrect due to insufficient small frequency step a step size of 0.05 Hz, has been used when the response of the optimized designs has been evaluated.

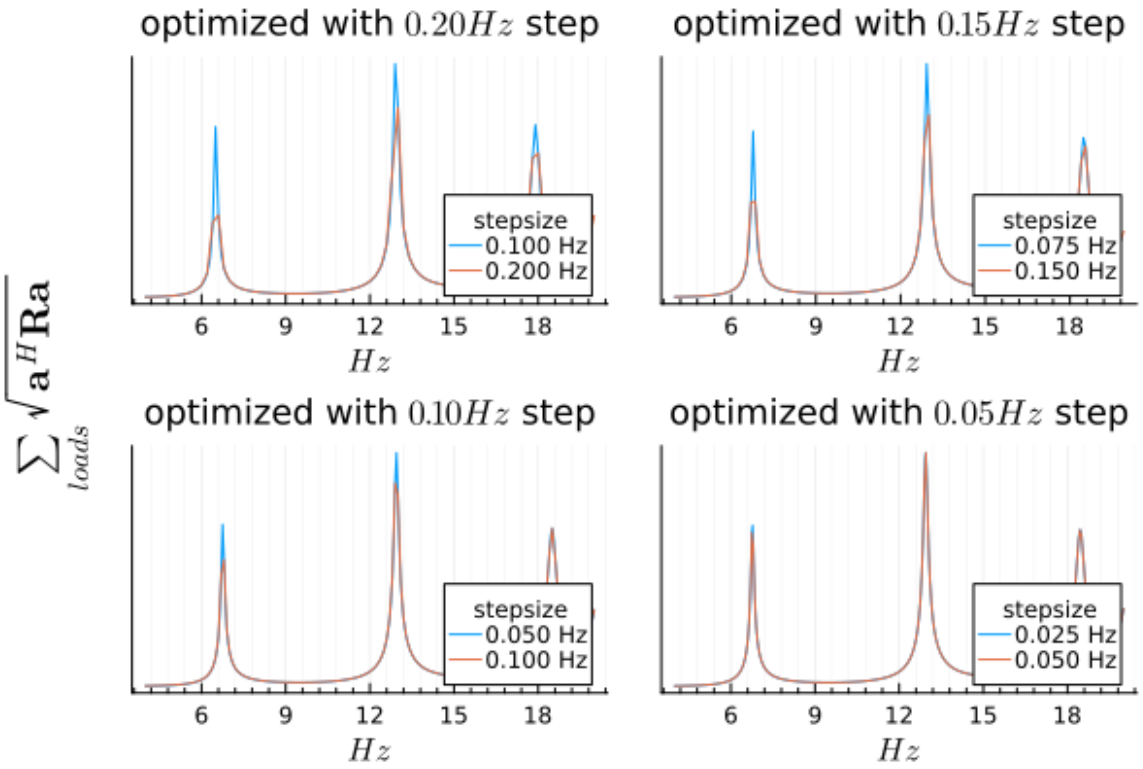

Figure 26: *Comparison of optimization results for different frequency step sizes. The orange curve is the step size optimized with; the blue curve is evaluated with half the step size and shows where peaks values are cut.*

B Penalization scheme

The purpose of the penalization scheme is to make intermediate values of the design variables unfavorable. To do so a SIMP-scheme is used, as described in Section 2.2.2, where the filtered designvariable is raised to a value of p, q, r respectively, when assembling the stiffness, mass and damping matrix. The penalization for this optimization has then three matrices to penalize, to narrow it down the penalization of the mass matrix q is set $q = 1$ since this corresponds to the physical interpretation and is expected to be of less importance since the density difference between the elastomer and wood is small, and that the mass of the elastomer layer has a minor contribution to the total mass. With the choice $q < p$, where p penalize the stiffness matrix, some kind of interpolation scheme may be needed, as the stiffness approaches zero faster than the mass, causing low frequency artificial eigenvalues to occur, this is described in for example (Pedersen 2000). Since the elastomer is modelled with one element thickness, this has not been considered here, since all dofs will obtain stiffness from the wood. The choice of r (damping matrix) is $r > 1$, so that the contribution to damping becomes lower than its contribution to the volume for intermediate values. For p, the physical choice would be $p > 1$ as the contribution to stiffness is zero unless the space between the wood panels is completely filled. Since low stiffness can be favorable to the objective, $p > 1$ gives a lower value of the objective and the intention to push the design variables to its boundaries may be reduced. Therefore, a choice of $p < 1$ might be favorable to obtain a black and white design. Different penalization schemes has been investigated and the evolution of the objective function are presented in Figure 27, where it can be seen that all three solutions with $r = 1$ fails to converge, indicating that the convergence is controlled by penalization of the damping matrix. Based on fast convergence and a stable optimization the values used are, $r = 2$ and $p = 1$.

The large oscillations for $p = 1$ and $r = 3$ in Figure 27, reins from that, in regions without elastomer, several modes where the wooden layers above and underneath the elastomer disconnects and oscillates in different directions appear.

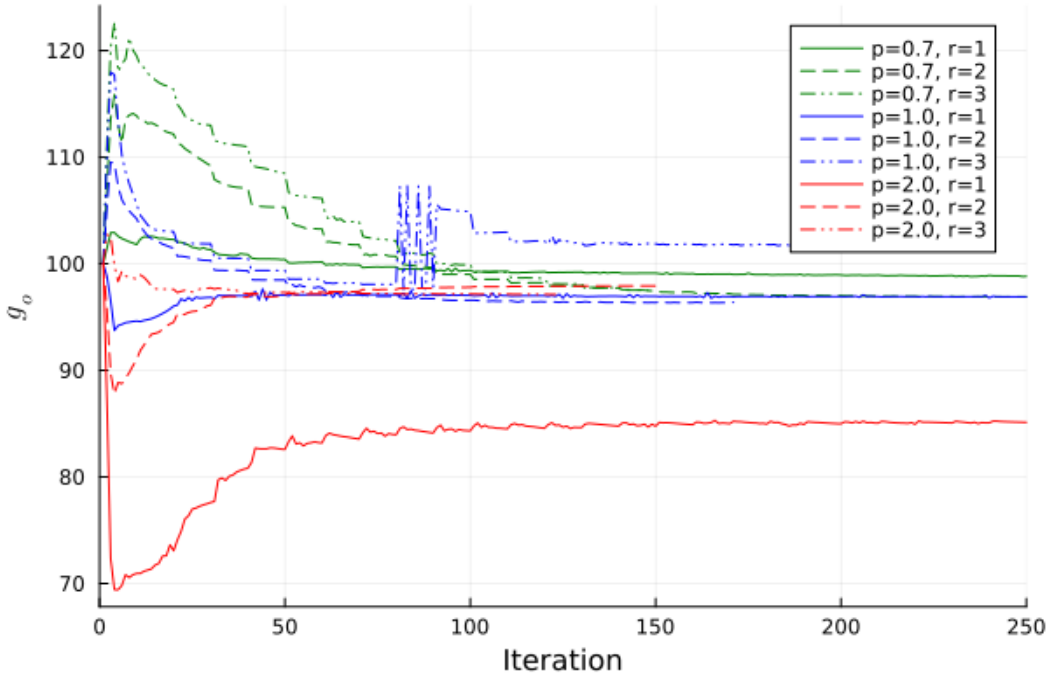

Figure 27: *Evolution of objective function for different penalization exponents*

C Applied load

When evaluating the dynamic response of a structure it is necessary to apply load in such a way that all modes of interest are triggered. For a panel where we are mainly interested in the response of modes orthogonal to its plane, mainly consisting of bending and torsional modes. A load spot which triggers all of those modes, is in one of the corners, if there are no prescribed displacement boundary conditions present. Optimizing with only a corner load may be problematic since the problem is then formulated as minimize the response for that load point without consideration of how the structure behaves when loading somewhere else. The computational time increase with the number of loads that is evaluated, since, for each load the objective function and its sensitivities needs to be evaluated. To find a loading situation that capture the dynamic response of the panel, four different load combinations has been investigated, where load is applied to a quarter of the panel because of symmetry. First one is to apply load as traction over a surface by dividing the quarter of the panel in 5×3 loading zones. This load combination is the one which may be considered to be most similar to real loading situation and may therefore be most robust. Second is a randomized load over the whole quarter, and third is four point loads. Drawing two lines at 1/6 and 1/3 of the panel length in each direction then the load is applied at the dofs closest to the intersection of these lines. This load is used and shown in Figure 8. The last load is a single load in a corner applied as traction over a surface of 0.1×0.1 m. This four different load combinations are evaluated of a frequency range from 5 Hz to 100 Hz. The designs are presented in Figure 28 Where all four designs show a similar pattern. The load used is 4 Point loads as this renders into a decent design, similar to the 5×3 traction load, while at the same time the number of evaluations of the objective and its sensitivities are not too large.

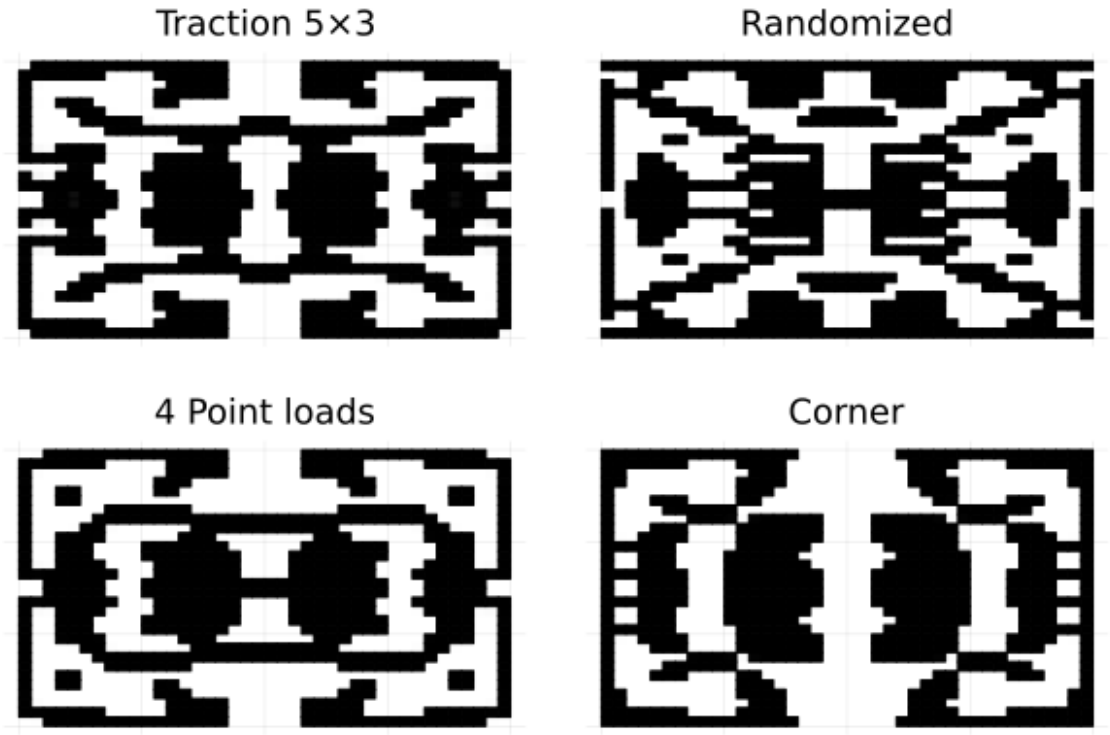

Figure 28: *Designs for different applied loads*

D Evaluation of approximated sensitivities

To evaluate the accuracy of the approximated sensitivities a 3 layer panel with 3464 dofs has been used to compare the sensitivities obtain when using modal analysis, to those obtained by solving the full system. The residuals $\mathrm{R_g}$ are defined as follows,

$$\mathrm{R_g} = \frac{||\frac{\partial g_f}{\partial \boldsymbol{\kappa}} - \frac{\partial g_r}{\partial \boldsymbol{\kappa}}||_2}{||\frac{\partial g_f}{\partial \boldsymbol{\kappa}}||_2}$$

where g_f is g evaluated by solving the full system and g_r is obtained when solving the reduced. R_g has been plotted in Figure 29 with different number of modes included in g_r. This error is larger around eigenvalues when setting the loss factor η to different values for the elastomer and wood. This may be a natural consequence since the damping in a structure controls the response around eigenfrequencies, and when the damping properties is allocated to the elastomer layer, the response around eigenfrequencies is controlled by the elastomer layer where the designvariables are implemented. As long as the number of modes included is sufficient to describe the objective, and the objective is successfully minimized, this error should not be of concern.

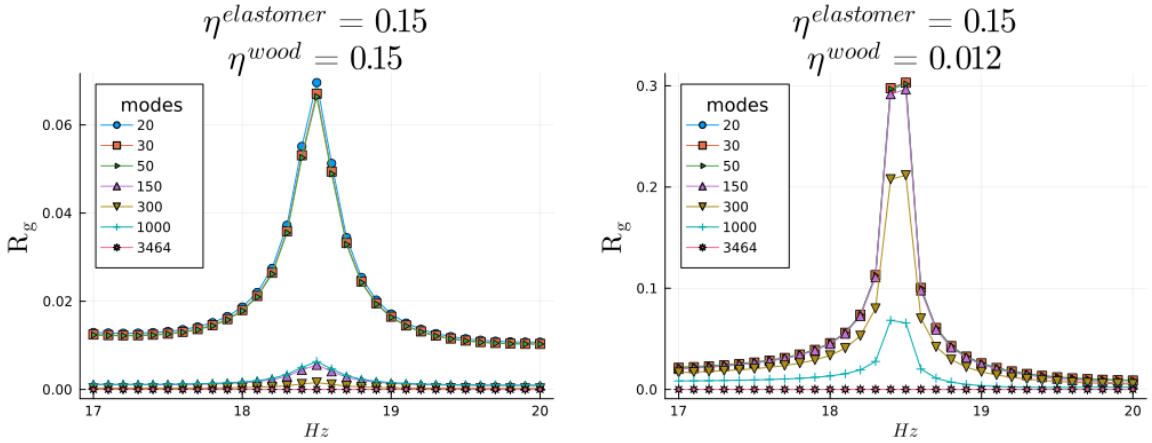

Figure 29: *Comparison of the error of approximated sensitivities for different number of modes included in the approximation. In the left figure wood and elastomer has the same loss factor, in the right figure wood and elastomer posses different loss factors.*